LDACS Flight Trials: Demonstration and Performance Analysis of the Future Aeronautical Communications System

Miguel A. Bellido-Manganell, Thomas Gräupl, Oliver Heirich, Nils Mäurer, Alexandra Filip-Dhaubhadel, Daniel M. Mielke, Lukas Marcel Schalk, Dennis Becker, Nicolas Schneckenburger, Michael Schnell

Abstract—The L-band Digital Aeronautical Communications System (LDACS) is a key enabler of the new air traffic services and operational concepts necessary for the modernization of the air traffic management (ATM). After its initial design, compatibility tests with legacy L-band systems, and functional demonstrations in the laboratory, the system is currently undergoing the standardization process of the International Civil Aviation Organization (ICAO). However, LDACS has not been demonstrated in flight yet. In this paper, we present the first in-flight demonstration of LDACS, which took place in March and April 2019 in southern Germany and included four LDACS ground stations and one LDACS airborne station. We detail the experimental setup of the implemented LDACS ground and airborne stations together with the flight routes, the conducted experiments, and the frequency planning to ensure compatibility with legacy systems. In addition, we describe the demonstrated ATM applications and the security measures used to protect them. Based on the obtained measurement results, we evaluate the LDACS in-flight communication performance for the first time, including the achieved communication range, the measured end-to-end message latency, and the LDACS capability to provide quality of service by effectively prioritizing safety-relevant data traffic. Furthermore, we use the in-flight received signal power to assess the applicability of a theoretical path loss model. These flight trials contribute to the final steps in the development of LDACS by providing its in-flight communication performance and by demonstrating: first, its correct functionality in a realistic environment; second, its capability of supporting ATM applications and the advanced security measures that can be used to protect them; and third, its spectrum compatibility with legacy systems. We conclude that LDACS is ready to support ATM operations and that LDACS frequency planning can safeguard legacy systems successfully.

Index Terms—L-band Digital Aeronautical Communications System (LDACS), flight trials, Air-Traffic Management (ATM), Air-Traffic Control (ATC), communication, navigation, surveillance (CNS), Post-Quantum Cryptography (PQC).

I. Introduction

AIR transport is seen as a key enabler of economic growth and development. In fact, 35% of world trade by value is carried by aircraft and around 4.3 billion passengers used air transport in 2018 [1]. Its importance is growing yearly, as reports forecast that the number of flights will increase in Europe by 53% from 2017 to 2040 in the most-likely scenario

The authors are with the Institute of Communications and Navigation, German Aerospace Center (DLR), Münchener Straße 20, 82234 Weßling, Germany (e-mail: {Miguel.BellidoManganell, Thomas.Graeupl, Oliver.Heirich, Nils.Maeurer, Alexandra.Filip, Daniel.Mielke, Lukas.Schalk, Dennis.Becker, Michael.Schnell}@DLR.de). Nicolas Schneckenburger was part of the team during the flight campaign (e-mail: nicolas.schneckenburger@gmail.com).

[2]. These growth numbers are taken from reports published before the COVID-19 pandemic. Although the impact of this pandemic on air transportation is very strong, air traffic growth is expected to resume very quickly in post-pandemic times. The expected continuous air traffic growth entails a significant challenge to the Air Traffic Management (ATM), which must be able to sustain and enable such traffic growth whilst further guaranteeing safety and the allocation of cost-effective environmentally-friendly flight routes.

However, current air-ground voice and data communications needed for ATM, e.g., between pilots and air traffic controllers, are already suffering from the increasing saturation of the VHF band in some regions of the world such as central Europe [3], [4]. In an initial screening of the Federal Aviation Administration (FAA) and Eurocontrol reported in 2007, no system operating at the time was found to satisfy all ATM requirements [5], which triggered worldwide research into the modernization of the ATM infrastructure including the introduction of new services and operational concepts as well as the development of new Communication, Navigation, and Surveillance (CNS) technologies. In Europe, the SESAR ATM Master Plan [6] foresees the transition to modern digital data communications for ATM, among others, through the development and implementation of the L-band Digital Aeronautical Communications System (LDACS). Internationally, LDACS is reflected in the Global Air Navigation Plan [7] of the International Civil Aviation Organization (ICAO), and is currently undergoing the ICAO standardization process.
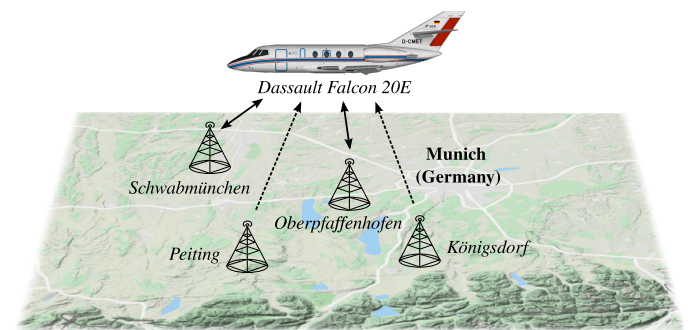

Fig. 1: LDACS flight trials using four LDACS ground stations deployed in southern Germany and one LDACS airborne station carried by a Dassault Falcon 20E aircraft. Two ground stations are full duplex and communicate with the airborne station bidirectionally. The other two ground stations only transmit and enable the airborne station to estimate its position using the LDACS ground station signals only. Copyright of map: Map data ©2020 GeoBasis-DE/BKG (©2009), Google.

The development of LDACS has already achieved important milestones: LDACS has been specified [8], evaluated through computer simulations [9] and laboratory tests [10], and its compatibility with other aeronautical CNS systems has been assessed [11]–[13]. In addition, LDACS draft Standards and Recommended Practices (SARPS) [14] have been endorsed by ICAO's Communications Panel. However, LDACS has not been demonstrated in flight trials and its performance has not been evaluated under realistic operating conditions.

In this paper, we present the first in-flight LDACS demonstration, which was conducted within the German project MICONAV (see Appendix B). In order to demonstrate the correct functionality of LDACS and its ability to support ATM communications and to incorporate advanced security mechanisms, we conducted several flight trials in March and April 2019 using an LDACS Airborne Station (AS) prototype carried by a Dassault Falcon 20E aircraft and four LDACS Ground Station (GS) prototypes deployed in southern Germany.

The correct functionality and operation of LDACS was tested by operating several emulated ATM applications over LDACS, such as Controller–Pilot Data Link Communications (CPDLC), Automatic Dependent Surveillance - Contract (ADS-C), Ground-Based Augmentation System (GBAS) communications, and, in general, audio and data communications. These applications were additionally secured using advanced security mechanisms: a secure key encapsulation procedure based on the asymmetric Post-Quantum Cryptography (PQC) McEliece scheme [15], [16] delivered a key for post-quantum robust symmetric data encryption to protect point-to-point communications, and the Timed Efficient Stream Loss-tolerant Authentication (TESLA) protocol [17] was employed to protect broadcast communications.

In addition, we used these flight trials to obtain the in-flight communication performance of LDACS under realistic operating conditions. Specifically, we obtained the achievable communication range and the message latency introduced by the data link, and evaluated the capability of LDACS to provide Quality of Service (QoS) by effectively prioritizing safety-relevant data traffic over low-priority data traffic. The obtained performance was also used to show that LDACS is able to support RCP400/A2[1], RCP240, and RCP130/A1 operations, as well as RSP400/A1[2] and RSP180/D surveillance operations, as required in the LDACS SARPS. The maximum data throughput achievable with the employed experimental setup was also measured in the laboratory and compared with the theoretical expectations. The flight trials also allowed us to assess the applicability of the Curved-Earth Two-Ray (CE2R) theoretical model by comparing the in-flight measured received signal power with the one estimated using the CE2R model.

The paper is structured as follows. We first provide a background on LDACS in Section II. Then, we describe the experimental setup in Section III and the conducted flights and experiments in Section IV. Afterwards, we show and assess the obtained results in Section V and provide our conclusions in Section VI.

II. LDACS BACKGROUND

LDACS is one of the radio access technologies realizing the future communications infrastructure that will allow aircraft to be connected to the Aeronautical Telecommunication Network (ATN) during all phases of flight. Specifically, LDACS shall connect aircraft operating in the continental airspace by deploying a cellular network of LDACS GSs, each one of them covering a part of the airspace denoted as an LDACS cell. An aircraft carrying an LDACS AS will then be able to connect to the ATN by joining the LDACS GS covering the airspace where it is operating. The aircraft will then communicate with the ATN through the GS until either a connection with another GS is more favorable and a handover to the new GS is conducted, or until the aircraft leaves the airspace covered by LDACS.

The ATN is an aviation-specific private wide-area network dedicated for communication related to flight safety and regularity. It supports multiple inter-networking protocols including the Internet Protocol (IP) that shall be used for LDACS. Additionally, it supports several other wireless access networks like satellite communications and VHF Data Link - Mode 2 (VDL-M2), which use non-IP legacy protocols.

Different types of aviation-specific standards are required for a new aviation communications system. These are to be developed by various standards development organisations. In particular, LDACS and ATN are under standardization by ICAO in collaborating teams. LDACS, specifically, is standardized within the project team "Terrestrial Data Link" (PT-T) under the Communications Panel since 2016 with a target applicability date of 2024. The ICAO activities have been supported by additional work within the Internet Engineering Task Force (IETF) [18] and the Single European Sky ATM Research (SESAR) program [8]. Particularly within SESAR, several dedicated sub-projects have been formed to increase LDACS's technology readiness level in collaboration with the industry. The output of these projects provides the basis for the LDACS standardization documents (SARPS and manuals) compiled by ICAO. In addition to the ICAO activities, Minimum Aviation System Performance Specifications (MASPS) and Minimum Operational Performance Standards (MOPS) need to be developed by the European Organization for Civil Aviation Equipment (EUROCAE) and the Radio Technical Commission for Aeronautics (RTCA), while avionics Form Fit and Function (FFF) specifications need to be developed by the Airlines Electronic Engineering Committee (AEEC). The latter activities are currently in preparation.

LDACS provides a bidirectional broadband radio link between airborne and ground stations capable of supporting data and voice communications with different QoS levels depending on the communication requirements of each application or user. This way, a wide variety of applications with different requirements can be supported by LDACS, such as Air Traffic Control (ATC) and Airline Operational Control (AOC) communications. In addition, LDACS may be used for command and control non-payload communications

---

[1]Required Communication Performance (RCP)
[2]Required Surveillance Performance (RSP)

e.g., to support single-pilot operations of equipped aircraft. Note that LDACS *must not* be used for communication *not* related to safety and regularity of flight since the use of the aeronautical L-band is restricted to the Aeronautical Mobile (Route) Service (AM(R)S) such as ATC and AOC.

ATC employs three data communication applications: CPDLC, ADS-C, and Context Management (CM) as defined by ICAO. Currently, CPDLC is used in tactical conflict management to issue basic clearances, e.g., for climb/descent, turns and headings, or sector handover. In the future, air traffic management shall shift towards pre-tactical conflict management. CPDLC will therefore be required to support trajectory-based operations based on complex clearances and 4D trajectory negotiations. Complex CPDLC clearances managing the flight trajectory are enabled by ADS-C downlinking the anticipated trajectory, called the extended projected profile, and CM providing automatic sector handovers. The deployment of pre-tactical conflict management is, however, stalled by the saturation of the VDL-M2 capacity by AOC data traffic in Europe [19]. In other parts of the world the current situation is not yet as severe.

AOC is the business communication of the airlines. As such, it differs from airline to airline. However, most airlines rely on data communication to uplink administrative and meteorological information to the flight crew, called the electronic flight bag, and to downlink flight performance data for predictive maintenance. AOC provides immediate economic benefits for airlines and is therefore heavily used.

In order to support future ATC and AOC applications, LDACS shall satisfy the performance requirements specified in the LDACS SARPS referencing the ICAO Performance-based Communications Manual DOC9869 [20] and EURO-CAE ED228A / RTCA DO-350A [21]. These performance requirements are defined using the RCP and RSP terminology, which define the set of system performance parameters that are required for a communications or surveillance system to support a communications or surveillance application, respectively. Thus, in order to support the ATC and AOC applications, LDACS shall comply with the communication performance definitions RCP400/A2, RCP240, and RCP130/A1, and with the surveillance performance definitions RSP400/A1, RSP180/D, and RSP160/A1 [14]. Each RCP and RSP definition implies a different latency requirement for the communication service provider, i.e., LDACS. We provide the required latency of each RCP and RSP definition when evaluating the obtained results in Section V.

LDACS operates in the aeronautical L-band between 960 and 1164 MHz. An LDACS cell employs a pair of frequency channels of 495.05 kHz each; one for ground-to-air communications, i.e., Forward Link (FL), and one for air-to-ground communications, i.e., Reverse Link (RL). The RL frequency is indicated in the FL GS broadcasts, which are searched for by the AS by iteratively scanning the possible FL frequencies. By using frequency-division duplexing, the FL and RL can be operated simultaneously, which drastically reduces the latency of the messages transmitted over LDACS. Additionally, in order to make an efficient use of the scarce spectrum available, the pair of frequency channels used by one cell can be reused by other distant cells. This frequency planning must also guarantee that legacy systems operating in the L-band, such as the Distance Measuring Equipment (DME), are not affected by the presence of LDACS. Up to now, such spectrum compatibility was only supported by theoretical studies [13] based on laboratory measurements [12]. Our flight trials represent the first real-world compatibility tests between LDACS and the legacy systems operating in the L-band.

Both the FL and the RL employ Orthogonal Frequency-Division Multiplexing (OFDM), with up to 50 active sub-carriers spaced 9.765625 kHz apart and a cyclic prefix of 17.6 μs. Adaptive coding and modulation is used to dynamically adapt transmissions to the changing link quality, which allows LDACS to make an efficient use of the spectrum and to achieve user data rates from 469 kbps up to 2819 kbps for a pair of FL and RL channels [8]. Time and frequency synchronization between the GS and the AS is achieved by employing the mechanisms described in the LDACS specification, which are mainly based on the use of a random-access frame, synchronization sequences, and pilot symbols. Whilst only the GS transmits in the FL of the cell, the RL is shared among all aircraft registered to the cell. A concurrent and reliable data transfer in the RL is provided by the GS, which dynamically allocates the RL resources for the different aircraft based on their data traffic demands. Specifically, the data-link layer of LDACS provides the necessary protocols to facilitate concurrent and reliable data transfer for multiple users.

LDACS has the potential to be developed into an integrated CNS system, as it does not only support communications, but can also enable navigation with a built-in ranging functionality [22] and might be used for non-cooperative surveillance applications [23]. Moreover, an air-to-air mode of LDACS is being researched on with the goal of extending LDACS coverage to the airspace that cannot be directly covered by ground stations [24], [25]. The navigation performance achievable using LDACS was measured in previous flight trials [26], [27]. Those flight trials focused solely on the LDACS navigation performance and employed GSs only capable of transmitting and an AS only capable of receiving. Consequently, no bidirectional real-time communications were performed and LDACS communication functionality was not demonstrated in those flight trials.

Currently, ATC and AOC utilize satellite communication systems mainly in oceanic, remote, and polar regions, and VDL-M2 is the preferred system for the continental airspace. Given that LDACS is also intended to support ATC and AOC in the continental airspace, we compare the main specifications of LDACS and VDL-M2. While LDACS is based on technologies employed by current mobile communication systems such as 4G, VDL-M2 was designed in the 1980ies and has known shortcomings. As we show in Table I, the two most important shortcomings of VDL-M2 are its low data rate and its lack of QoS support and data traffic prioritization. First, VDL-M2 employs differential 8-ary phase shift keying modulation with a rate of 31.5 kbps. In practice, the user data throughput lies below this value, as the overhead data for synchronization and redundancy also need to be considered. In

TABLE I: Comparison between LDACS and VDL-M2 technologies.

	LDACS [8]	VDL-M2 [28]
Operating frequency	960-1164 MHz	117.975-137 MHz
Channel bandwidth	495.05 kHz (FL) + 495.05 kHz (RL)	25 kHz
Channel access	Contention-free	Contention-based CSMA
Maximum user data throughput	2818.7 kbps	< 31.5 kbps
QoS with traffic prioritization	Yes	No
Operation	Full duplex	Half duplex
Standardization	Draft [14]	Completed [28]
Already deployed	Experimental only	Yes

addition, the contention-based Carrier-Sense Multiple Access (CSMA) channel access employed by VDL-M2 reduces the practically achievable data rate considerably, as the maximum throughput is already reached at approximately 40% channel utilization [29]. The impact of the low achievable data rate is aggravated by VDL-M2's lack of QoS mechanisms. Since no priority mechanism is in place, higher volume AOC data traffic can starve out ATC data traffic. As we can see in Table I, LDACS was designed to provide a much higher user data throughput and to support QoS and data prioritization. In addition, the full-duplex operation of LDACS and its GS-scheduled contention-free medium access, which combines time-division and orthogonal frequency-division multiple access, allows to maximize the throughput and the channel utilization and to reduce the end-to-end message latency. Thus, LDACS is expected to be able to support all applications currently supported by VDL-M2, in addition to new applications and operational concepts required for the ATM modernization. This comes at the cost of operating in a frequency band already utilized by other systems, which imposes the need for compatibility tests between LDACS and the other legacy systems. Moreover, although the current deployment of VDL-M2 makes it a more desirable solution for some institutions to cope with the increasing data traffic demands in the short term by using additional VHF channels, it is generally agreed that a high-throughput and QoS-supporting solution operating outside the VHF band, such as LDACS, will be needed in the medium or long term. In some regions like Europe, where the VHF band is already saturated [19], LDACS might be needed even in the short term.

The main objectives of the flight trials and the experiments are as follows. First, we want to confirm that LDACS can operate as described in its specification and that the procedures defined for its operation, such as cell entry, cell exit, and handover between cells, can be conducted correctly. Second, we want to measure the in-flight communications performance of LDACS, including its communications range and data latency, and verify its QoS support and data prioritization. Third, we want to verify that LDACS can support the secure exchange of data from ATC and AOC applications and that the RCP and RSP criteria specified in the LDACS SARPS can be fulfilled. Finally, we want to test whether LDACS can operate in the L-band without interfering other systems if an appropriate frequency planning is applied.

Fig. 2: Simplified experimental setup, with four GSs and one AS. Two GSs are full duplex, i.e., can communicate bidirectionally with the AS, which is also full duplex, and two GSs can only transmit to the AS but not receive from it. The LDACS radio of each full duplex station is connected through a UDP/IP interface to a computer running the ATM applications and implementing the security measures used to protect the applications. Moreover, each computer manages and monitors the operation of the LDACS radio and generates additional synthetic data traffic used for performance evaluations. The components of the experimental LDACS radios can be found in Fig. 3.

III. EXPERIMENTAL SETUP

A. Ground Stations and Airborne Station

In order to realistically recreate the future LDACS operational environment, we developed an experimental setup consisting of one AS, four GSs, and several computers generating data to be communicated using LDACS. The GSs were deployed in southern Germany on the coordinates shown in Table II. They covered adjacent and overlapping airspace volumes, as expected in the future LDACS cell deployment, although at smaller distances to keep the experiments manageable. The AS was installed in the DLR Dassault Falcon 20E (D-CMET) aircraft shown in Fig. 1, with the L-band antenna used by LDACS located in a port-hole at the bottom of the aircraft between its wings. The experimental setup is shown simplified in Fig. 2, where the components of the four GSs and the AS, as well as the communication links between them, can be seen.

Table II shows information about the deployed GSs, including the LDACS antenna altitude and the employed FL and RL frequencies. Out of the four GSs, two were full duplex,

TABLE II: Information about the deployed LDACS GSs. LDACS antenna elevation given above mean sea level.

| Identifier | Functionality | Location | Coordinates | Distance (km) to | | | Antenna elevation (m) | EIRP (dBm) | Frequency (MHz) | |
				GS-SM	GS-PT	GS-KD			FL	RL
GS-OP	Full duplex	Oberpfaffenhofen	48.084777 N 11.277793 E	43.5	45.2	31.8	605	40	994.0	965.5
GS-SM	Full duplex	Schwabmünchen	48.180160 N 10.709135 E	0	48.2	68.7	555	40	1001.5	966.5
GS-PT	Transmit-only	Peiting	47.765949 N 10.901001 E	48.2	0	43.0	750	40	992.5	-
GS-KD	Transmit-only	Königsdorf	47.8289269 N 11.469345 E	68.7	43.0	0	603	40	1000	-

namely GS-OP and GS-SM, and two were transmit-only GSs, namely GS-PT and GS-KD. Each full duplex GS employed a complete LDACS GS radio, implementing both a transmitter and a receiver, based on the LDACS specification [8] and fulfilling the LDACS draft SARPs from ICAO [14]. Thus, it set up its own LDACS cell and was able to communicate bidirectionally with the AS. In contrast, a transmit-only GS implemented only a transmitter and consequently could only transmit data to the AS but not receive any data from it.

The AS employed a complete LDACS AS radio based on the LDACS specification [8] and fulfilling the LDACS draft SARPs from ICAO [14]. It could therefore communicate bidirectionally with any full duplex GS and additionally receive the transmissions from the transmit-only GSs.

The reason for this experimental setup is that only two full duplex GSs and one full duplex AS are needed to test the LDACS communication functionality including procedures such as cell entry, cell exit, and handover between cells. The two transmit-only GSs transmitted pseudo-random data and have been solely deployed to allow the AS to estimate its position by analyzing the signals transmitted from four GSs. To this end, the AS implemented an additional receiver used solely for LDACS-based position estimation.

The components of the experimental full-duplex GS and AS prototypes used in the flight trials are shown in Fig. 3. Each station employed a Global Navigation Satellite System (GNSS) receiver[3] and an atomic Rubidium clock[4] to obtain an accurate GNSS-disciplined time and frequency reference for the LDACS radio and IQ-data recorders[5]. This also allowed the GSs to be finely time synchronized with each other such that their transmit signals could be used by the AS for precise position estimation. The components of the RF front end of the LDACS radio, i.e., the diplexer, the receive Low-Noise Amplifier (LNA) and transmit High-Power Amplifier (HPA), as well as the receive and transmit band-pass filters, were customized by the company *BPS GmbH* for the LDACS experimental prototypes. The receiver and transmitter modules supporting the LDACS stack were implemented by *iAd Gesellschaft für Informatik, Automatisierung und Datenverarbeitung mbH* using the *R&S WFDE-DU5010* development platforms. The stations employed a blade-style vertically-polarized L-band
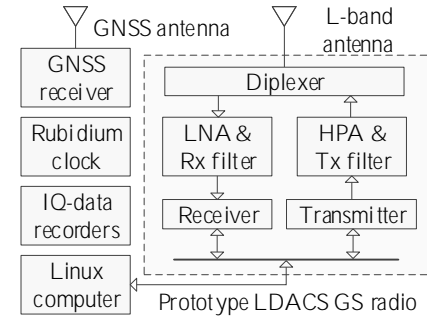
Fig. 3: Components of the experimental full-duplex GS prototype. The experimental AS prototype comprised the same components with an additional receiver path used solely for navigation purposes.

antenna[6] with nominal omni-directional radiation in azimuth and co-sinusoidal in elevation, achieving an approximate maximum antenna gain of 5 dBi. Note that antennas with different shapes might be used in the future by the LDACS ground stations. Although this could lead to different antenna radiation patterns, it is not expected to change the results presented in this paper. The impact of the maximum antenna gain on the performance of the system is discussed in Section V-C.

As one of the objectives of the flight campaign was to demonstrate the LDACS capability to support ATM-relevant applications and to assess its communication performance under real operating conditions, our experimental setup emulated the presence of future end-users running such applications. This was achieved by running the applications of interest on computers connected to the stations and by using LDACS to exchange the data generated by the applications. The application data generated by the airborne computer were passed on to the LDACS AS radio using a UDP/IP interface and transmitted to the connected full duplex GS using LDACS (see Fig. 2). Then, the receiving GS processed the received signal and passed the received data on to the GS computer using a UDP/IP interface. Finally, the application receiving the data processed the received information and reacted accordingly.

B. Applications

Four different aeronautical applications were demonstrated during this flight campaign. First, CPDLC was emulated by exchanging short text messages between the computer connected to the AS and either the GS-OP or the GS-SM computer. These messages included standard commands and responses as used in CPDLC. Second, the ADS-C service was recreated

---

[3] *Septentrio PolaRx4TR^{PRO}*
[4] *Spectratime LNRClok-1500*
[5] Multiple devices, including the *R&S EX-IQ-BOX*, *R&S IQR 100*, and *R&S TSMX-PPS 2*, as well as a customized IQ-data recorder module using *National Instruments PXI Series* devices.

[6] *Sensor Systems S65-5366-10L*

by periodically transmitting the position of the aircraft from the AS computer to either the GS-OP or the GS-SM computer. Third, the transmission of audio messages was demonstrated by transmitting from the AS computer several prerecorded audio messages to the GS-OP computer. The audio messages had to be prerecorded due to the noisy environment of the test aircraft. Fourth, correction data from an experimental GBAS deployment at the German Aerospace Center (DLR) site in Oberpfaffenhofen [30] were collected by the GS-OP computer and sent to the AS computer using LDACS. Using the correction data provided in the GBAS messages, the aircraft can estimate its GNSS-based position much more accurately and with a higher integrity level, allowing it to perform complex ATM procedures not feasible otherwise [31].

C. Security

In order to test the transmission of secured applications using LDACS, the data generated by the demonstrated applications were secured prior to their transmission. The implemented security architecture was based on the architecture proposed for LDACS in [32]. However, since the security architecture was not yet part of the LDACS specification at the time of prototype development, the security protocols were implemented in the application layer (see Fig. 2). Two different security mechanisms, proposed for LDACS in [33], were implemented to secure first the applications using point-to-point communications, i.e., CPDLC, ADS-C, and audio transmission, and second the applications using broadcasts, i.e., GBAS.

After the AS successfully joins a cell, and prior to any exchange of point-to-point user data, a secure key exchange procedure based on the asymmetric PQC McEliece scheme [15], [16] is conducted between the AS and the GS to guarantee their mutual authentication and a secure key exchange between them. This is achieved firstly by exchanging the public McEliece keys of both participants in a secure manner, secondly by authenticating each other, and finally by conducting an authenticated PQC key exchange. After this point, all later point-to-point user data communications, including CPDLC, ADS-C, and audio transmissions, are protected by an AES[7]-256 encryption scheme in Galois Counter Mode [34], [35], providing at least 128-bit security levels [36] and ensuring data confidentiality, integrity, and authenticity.

GBAS was secured by using the broadcast authentication protocol TESLA [17]. Basically, the sender, i.e., GS-OP, divides time in equal intervals, employs a self-authenticated chain of keys, applies a key to each time interval, and uses the key of that interval to calculate a Message Authentication Code (MAC) over every broadcast message sent in that interval. The broadcast message, its MAC and a key from a previous interval are then broadcast using LDACS. The receivers, i.e., the AS, receive and buffer each message, MAC and key, and wait for the correct key to verify the MAC. This way, the receivers can be sure that the message was transmitted by the legitimate sender, i.e., GS-OP, as no one else knew the key for the MAC calculation at a previous time. Together with the verification of

---

TABLE III: Synthetic data traffic patterns.

Traffic pattern	Data load	Packet sizes (bytes)	Proportions	Priorities
T1	100 kbps	1400 / 1400	50% / 50%	High / Low
T2	100 kbps	175 / 1400	70% / 30%	High / Low

the authenticity of the sender and this mechanism, we secured the integrity and authenticity of all GBAS messages sent using LDACS, as well as the trustworthiness of their origin.

By securing the applications using these security measures, the aim was to demonstrate that LDACS is capable of not only supporting different aeronautical applications under real-life conditions, but also securing them robustly using state-of-the-art security measures providing PQC security levels.

D. Synthetic Data Traffic

The computer of each station generated additional synthetic data traffic following predefined data traffic patterns that realistically represent the behavior of additional sets of applications. This allowed us to recreate the data traffic expected to be communicated through LDACS in the future and consequently to assess the LDACS capability to support ATM-relevant applications under realistic system load conditions. Additionally, using different traffic patterns allowed us to analyze the LDACS performance when packets with different sizes and priorities are transmitted and, consequently, to assess if LDACS can effectively support different quality of service levels. Strict prioritization is a highly desirable quality of service feature for a communication system that shall be used to convey safety-related messages. The LDACS protocol has therefore been designed to support priority-based medium access via centralized resource scheduling, and to avoid head-of-line blocking through the support of transparent message fragmentation.

The two synthetic data traffic patterns tested in the flight campaign are described in Table III. For both traffic patterns, a data load of 100 kbps was generated by each computer and passed on to the connected LDACS radio to be transmitted using the acknowledged LDACS transmission mode, in which the transmitter requests an acknowledgment from the receiver for each transmitted message. Since the traffic pattern is generated by each sender, it is actually carried twice over the LDACS data link. Once in each direction. The time between generated packets was distributed exponentially according to the offered load and packet sizes. For the traffic pattern T1, packets of 1400 bytes were generated and marked with high and low priorities in equal proportions in terms of offered load. The traffic pattern T2 was composed of a larger number of small high-priority packets, representing ATC messages, and few large low-priority packets, representing for example AOC messages. Therefore, the T2 scenario recreated the future operational environment of LDACS where a part of the data traffic might be safety-relevant, e.g., ATC data, and must be prioritized over other data, e.g., AOC data.

In addition to generating synthetic data and the data from the running applications, each computer managed and monitored the operation of its connected LDACS radio by sending com-
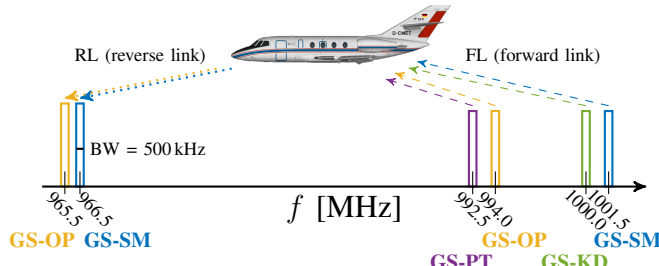
---

[7]Advanced Encryption Standard (AES)

Fig. 4: LDACS FL (dashed arrows) and RL (dotted arrows) frequencies used in the LDACS demonstration setup.

mands to and receiving operational logs from it, respectively, as shown in Fig. 2.

E. Frequency Planning

An LDACS cell employs two frequency channels in the L-band: one for the GS transmissions in the FL and one for the AS transmissions in the RL. The frequencies employed for each LDACS cell in our demonstration setup are listed in Table II and depicted in Fig. 4. Note that, whilst a GS only operates using the pair of FL and RL frequencies used in its cell, the AS must be able to join different cells and, therefore, must be able to switch between different pairs of frequencies. Furthermore, the additional receiver used in the AS for LDACS-based position estimation was able to receive the entire FL band, i.e., the four FL frequencies used in our measurement setup, in order to estimate the position of the aircraft by analyzing the signals transmitted by all GSs.

The frequencies used in the flight campaign were chosen based on the frequency planning strategy described in [13]. Such frequency planning allowed us to determine the conditions, such as transmit frequency and transmit power, under which an LDACS station could operate in a certain location with no impact on legacy systems such as DME. Figure 5 displays the positions of the DME transponders (DME ground stations) operating in the area of interest, as well as the positions of the four LDACS GSs. Note that the frequency planning allowed us to locate the LDACS GSs in the chosen positions despite the presence of many DME transponders close to the city of Munich, particularly around its international airport. To grasp the complexity of the conducted frequency planning, Fig. 6 shows the distance between the LDACS GS-OP and the closest DME transponder using a certain frequency for transmissions or receptions, i.e., transmissions from airborne DME interrogators. Note that, whilst no DME frequency is used within the RL band (depicted in yellow), many DME stations use frequencies falling within the FL band (depicted in green) employed in the campaign. Moreover, some of those frequencies are actually employed by DME transponders located nearby. For example, DME transponders located 51, 89, 134, and 81 km away from the GS-OP transmit at 993, 995, 997, and 999 MHz, respectively. Another interesting example of the resulting frequency planning is the DME transponder using the 1003 MHz frequency and located at the Oberpfaffenhofen airport only 2 km away from the GS-OP. Despite their closeness in distance and frequency to the LDACS GSs, the geometrical and power-
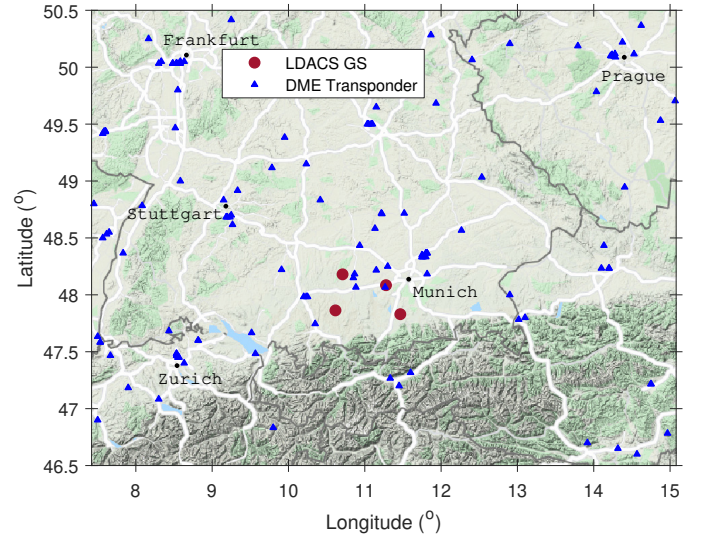
Fig. 5: Locations of the LDACS GSs and the DME transponders in the area of interest. Copyright of background map: Map data ©2020 GeoBasis-DE/BKG (©2009), Google.
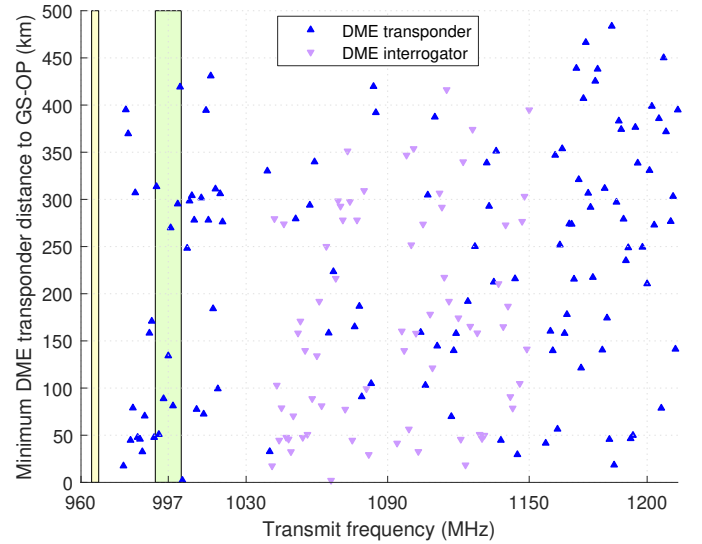
Fig. 6: Distance between the GS-OP and its closest DME transponder employing a certain frequency for transmissions or receptions. The experimental LDACS frequency bands used in the campaign are shown in yellow (RL) and green (FL).

based considerations taken in the frequency planning ensure that no DME station (transponder or interrogator) would be affected by LDACS transmissions, as the desired-to-undesired signal power ratio experienced by the DME receivers would always stay above a certain robustness threshold.

F. Limitations of the Experimental Setup

In order to comply with regional regulations, the average Equivalent Isotropically Radiated Power (EIRP) of each GS was limited to 40 dBm as compared to the maximum EIRP of 52 dBm defined by the LDACS SARPs. The GSs were located closer to each other, compared to a real deployment, to keep the experiments manageable. In addition, due to limitations of the prototyping platform, the RL resources allocated to the AS

were limited to a maximum of 110 tiles per RL multiframe[8], which increased the transmission latency during traffic peaks. Moreover, only the most robust coding and modulation scheme was employed in both the FL and the RL throughout the campaign. This mainly entails using QPSK modulation in both the FL and the RL, as well as a concatenated code (convolutional coding coupled with block interleaving and Reed-Solomon coding) with a coding rate of 0.45 for the FL common control and user data, and of 0.44 to 0.42 for the RL user data. Although this constraint made communications more robust against impairments, it also prevented the LDACS demonstration setup from reaching a higher data throughput and a lower packet latency by adapting the coding and modulation scheme to the link state, as described in the LDACS specification [8] and expected in the future LDACS operation.

IV. FLIGHTS AND EXPERIMENTS

A total of six flights were conducted over a period of two weeks in March and April 2019. The aircraft always took off and landed at the airport located next to the premises of the DLR in Oberpfaffenhofen, close to the city of Munich, Germany. As the OP-GS was located directly on the DLR premises, additional experiments could be conducted before take-off and after touchdown with the aircraft on the apron and runway.

In general, the same schedule was followed for each flight. First, all stations were started with the aircraft still on the apron on pre-departure and initial communication tests were conducted between the AS and the GS-OP, which could communicate in these conditions with the AS even though some obstacles, including a hangar, blocked the radio Line of Sight (LoS) between both stations. After ensuring that the LDACS experimental setup was working correctly, clearance was given to the aircraft crew for take-off. Then, the aircraft carrying the AS flew the predefined flight route and the designed tests and experiments were conducted.

The routes flown by the aircraft and the reached altitude are depicted in Fig. 7. A total flight time of 12 hours and 54 minutes was accumulated and 8105.8 km were covered. After some of the flights, additional tests and experiments were conducted after landing with the aircraft on the apron or runway. During the tests conducted with the aircraft on the apron, the LoS between the AS and the GS-OP was blocked by several buildings. Given that these conditions of blocked LoS between an on-ground aircraft and a GS located nearby might be experienced in reality at some airports, these tests were of special interest in this campaign.

The tests conducted during the flight campaign have been grouped into 28 different experiments, described in Appendix A. The different experiments were aimed at testing the many aspects to be evaluated during the campaign, such as the LDACS capability to support ATM applications, the LDACS performance when fed with various data traffic patterns, the correctness of different LDACS procedures, e.g., handovers between GSs, and the achievable communication range with

---

the limited transmit power. Whilst most experiments were conducted in flight, experiments 1, 9, 22, and 25 took place with the aircraft on the apron.

V. RESULTS

A. LDACS Operation

The LDACS operation was tested in all experiments throughout the campaign. In addition to the data exchange between the AS and the GSs, the LDACS operation included many procedures defined in the LDACS specification that enabled this data exchange, such as cell entry, cell exit, and handover between GSs. These procedures were tested and demonstrated repeatedly throughout the flight trials, as the AS had to join and leave at least one cell in each experiment in order to exchange data with a GS. Handovers between the GS-OP and GS-SM were demonstrated successfully throughout the flight trials and with special emphasis during the fifth flight as shown in Fig. 8, where the data exchange between the AS and the GSs is depicted in different colors. One can see that the AS performed periodic handovers between both cells to exchange data with each GS alternatively.

B. Applications and Security

The applications described in Section III were demonstrated several times during the flight campaign (see Table V in Appendix A) and worked correctly. The security measures used to protect the applications were applied successfully and no disruptions were observed in this respect. This means that the key exchange procedure successfully resulted in the secure exchange of an AES-256 Galois Counter Mode session key. Then, all following point-to-point data communications between AS and GS were thus protected in terms of confidentiality and integrity using this 256-bit session key. A duration for the key exchange procedure of 283.74 ms for the 95th percentile was measured. This goes in line with the theoretical and simulation-based evaluations published in [37], [38]. An in-depth analysis of the security measures employed in the campaign for data broadcast over LDACS can be found in [31]. Consequently, LDACS was not only capable of supporting the correct operation of such applications, but it also provided enough data throughput to support the advanced security measures demonstrated in this campaign.

For example, the AS crew and the GS-OP crew exchanged CPDLC free-text messages throughout the flight trials. This was used not only to demonstrate the correct operation of CPDLC over LDACS, but also to coordinate the tests during the flight trials and to report the AS status. This allowed us to rapidly react to unexpected circumstances and to perform the tests more efficiently. Some of the actual CPDLC messages exchanged between the AS and the GS-OP during the flight trials are depicted in Fig. 9. As these communications were secured as described in Section III-C, the plain text shown in Fig. 9 could only be seen by the legitimate transmitter (the AS or GS-OP computer) and receiver (respectively the GS-OP or AS computer).

Another example of the demonstrated applications was the use of the ADS-C messages transmitted by the AS to the

---

[8]A RL multiframe comprises one synchronization tile, one automatic gain control preamble, and 160 tiles for dedicated control and data.
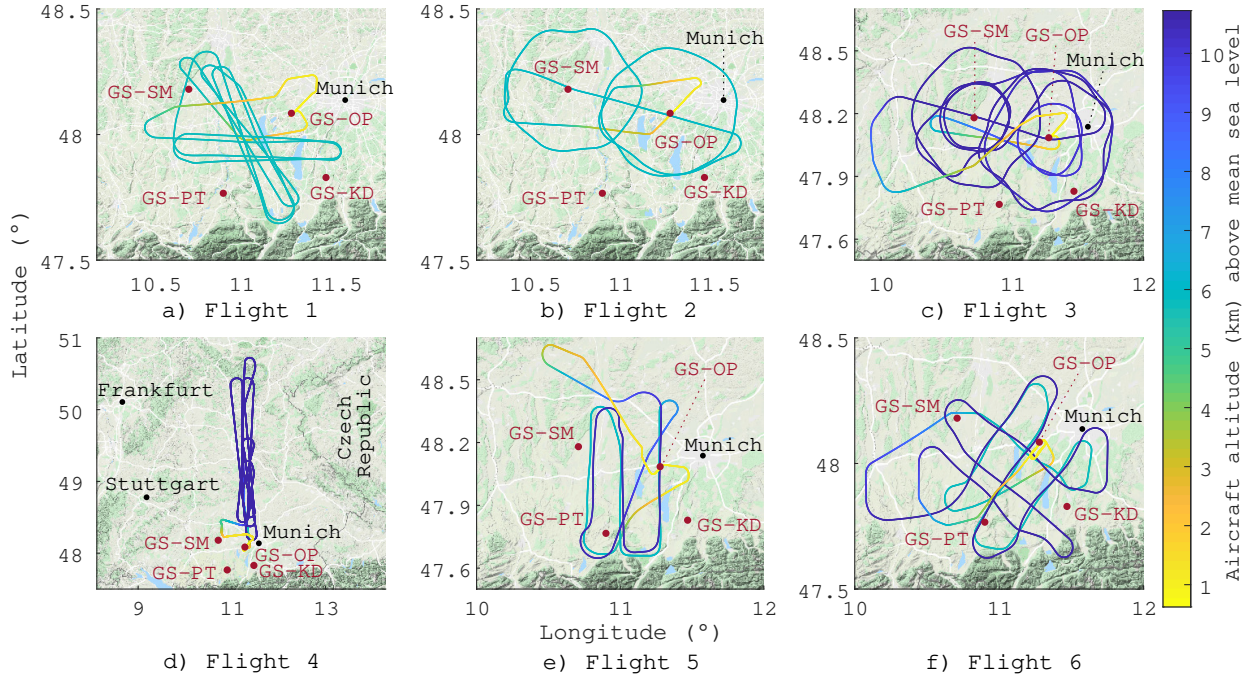
Fig. 7: Flight routes. The lines show the GNSS-based position of the aircraft during the flights and the line color indicates the aircraft altitude over mean sea level. Note that, given the high aircraft altitude, a good visibility to numerous GNSS satellites was available throughout the flights, which allowed for a robust position estimation. The locations of the GSs are labeled and marked in red. Copyright of background map: Map data ©2020 GeoBasis-DE/BKG (©2009), Google.
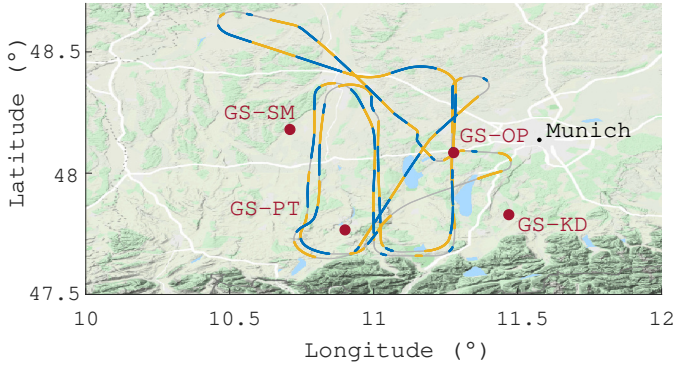

Fig. 8: Handover tests during the fifth flight. The AS exchanged data with the GS-OP (yellow) and with the GS-SM (blue) alternatively, performing handovers to switch between both GSs. The segments with no active connection are depicted in gray. Copyright of background map: Map data ©2020 GeoBasis-DE/BKG (©2009), Google.

GS-OP to display the live aircraft position and additional information in the GS-OP control room during the flight trials. Figure 10 shows an example of this representation. The GS-OP crew could see the live aircraft position, identifier, flight level, heading, and speed displayed on a map, together with the flown track and the indicators of the airports and aerodromes located nearby. All the information related to the aircraft status was contained in the ADS-C messages transmitted by the AS and received by the GS-OP. Having such a representation of the aircraft information on a map allowed us to coordinate and monitor the tests more efficiently throughout the flight trials, as well as to demonstrate a direct use of the ADS-C messages transmitted over LDACS. Note that all ADS-C messages were secured as described in Section III-C, which prevented any entity besides the legitimate receiver (the GS-OP) from being able to know the transmitted aircraft information, e.g., its live

position.

Moreover, we show in Fig. 11 the end-to-end latency of the application messages transmitted by the AS in flight and received by one of the GSs during the T2 scenario (experiments 7, 10, 12, and 13). Figure 11 additionally depicts the latency percentiles of two groups of application messages clustered according to their size: smaller application messages with a size between 280 and 300 bytes (blue dotted lines), and bigger application messages with a size between 1790 and 1810 bytes (green dashed lines). One can see that the smaller application messages are communicated with a latency lower than 0.08 s in more than half of the cases, and lower than 0.38 s in 99% of the cases. As expected, the bigger application messages present a higher latency, which however remains below 0.37 s in the majority of cases and below 1 s in 99% of the cases. Even in 99.9% of the cases, the latency remained below 0.8 s and 1.2 s for the smaller and bigger application messages, respectively. Whilst we can already see in Fig. 11 the crucial role of the size of a message in its latency, a more detailed analysis is performed in Section V-E.

We now compare the obtained message latency with the RCP and RSP requirements specified in the LDACS SARPS. The results confirm clearly that LDACS is able to support RCP400/A2, RCP240[9] and RCP130/A1 operations as defined in [21] or [20], which require the Required Communication Technical Performance of the Communication Service Provider $RCTP_{CSP}$, i.e. the LDACS radio, to be lower than 10 s, 100 s, and 10 s in the 95th percentile, respectively. RSP400/A1 and RSP180/D surveillance operations are also supported by these results, since they require a data delivery

---

[9]This is defined as RCP240/A1 in [21] and as RCP240/D in [20]. However, both definitions share the same requirements of interest.
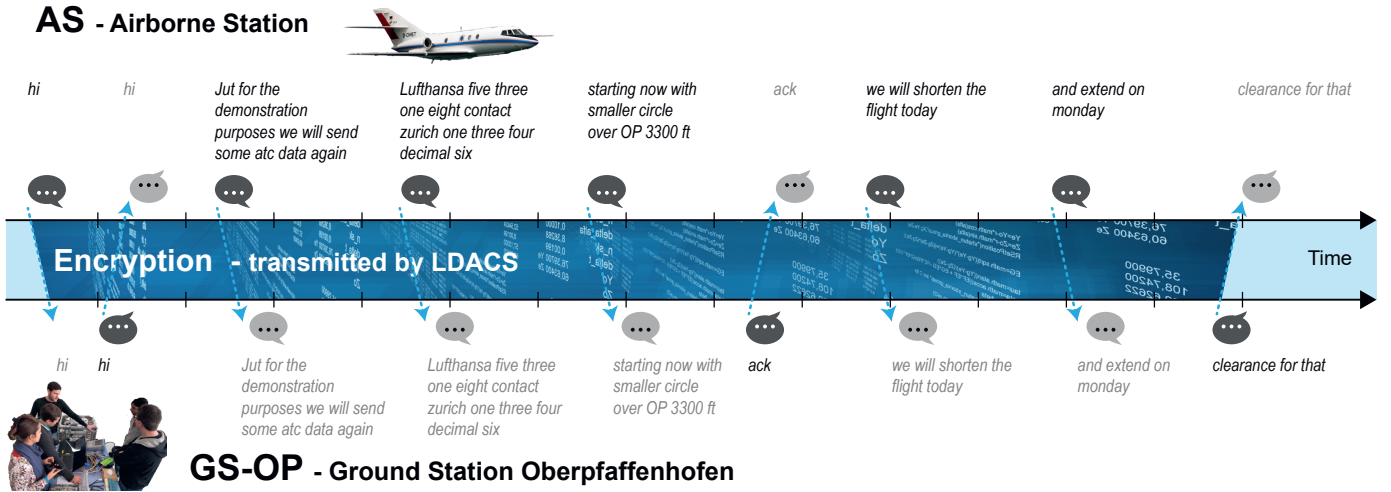
Fig. 9: Some CPDLC free-text messages actually exchanged between the AS and the GS-OP during the flight trials. As these messages were transmitted over LDACS encrypted, the plain text was only observable by the legitimate transmitter and receiver. Note that the plain text is depicted dark at the transmitter and light at the receiver.
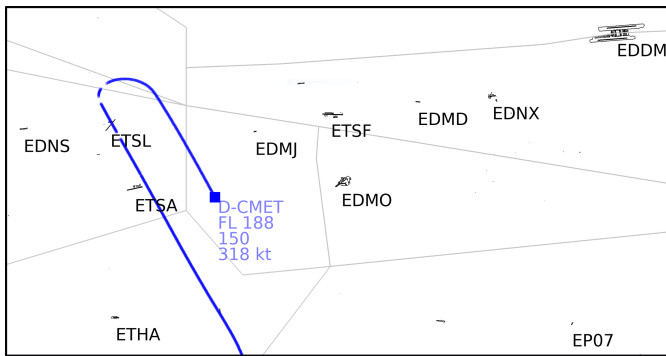

Fig. 10: The content of the ADS-C messages transmitted by the AS and received by the GS-OP during the flight trials was used to depict the live aircraft position, identifier, flight level, heading, speed, and track on a map in the GS-OP control room. Among others, this live information (depicted in blue) helped the GS-OP crew to coordinate and monitor the tests throughout the flight trials. Some context was added to the map by representing the position of airports and aerodromes located nearby, such as the Munich international airport (EDDM), the Oberpfaffenhofen airport (EDMO), and the Schwabmünchen aerodrome (EDNS), where the GS-SM was located.

time of less than 270 s and 84 s in the 95th percentile, respectively. The less restrictive 99.9th percentile latency requirement was also fulfilled for all considered RCPs and RSPs. As these operations are required in the LDACS SARPs [14], giving evidence that LDACS can support them represents a major result of this campaign. Note that the RSP160/A1 latency requirement of 5 s in the 95th percentile was also fulfilled. However, as no route prediction data were exchanged during the experiments, the support of RSP160/A1 operations could not be fully verified from our results.

C. Communication Range

In order to measure the communication range achievable with LDACS, the aircraft flew several times northwards and southwards over Germany during the forth flight, as shown in Fig. 7d. This allowed us to measure repeatedly the distance at which the AS lost the connection with the GS and was not capable of joining the cell and exchanging data with the GS anymore. Figure 12 shows the distances at which
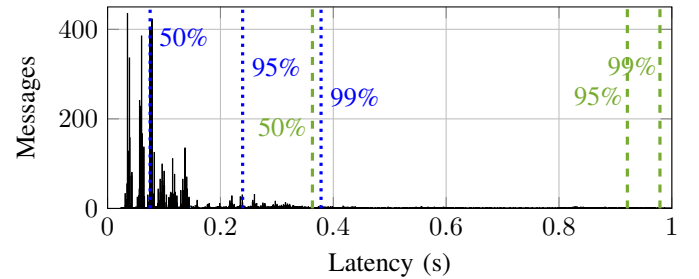
Fig. 11: Histogram of the latency of 7837 application messages transmitted by the AS in flight during the T2 scenario (experiments 7, 10, 12, and 13). The lines depict the 50th, 95th, and 99th latency percentiles of the application messages of 290 ± 10 bytes (blue dotted lines, 85.2% of the application messages) and of 1800 ± 10 bytes (green dashed lines, 13.6% of the application messages).

messages were successfully or unsuccessfully transmitted by the AS to the GS-SM for three different flight segments where the aircraft flew either away from the GS-SM (Fig. 12a and Fig. 12c) or towards it (Fig. 12b). Additionally, Fig. 12 shows the join and part events that took place during the flight. A join event represents a cell entry, i.e., the successful registration of the AS in the cell controlled by the GS and the allocation of RL resources for the AS to convey user data. On the contrary, in our experimental setup, a part event happens when one station (either AS or GS) assumes that the connection with its counterpart is over, not necessarily having to exchange any further data to communicate the disconnection. Therefore, each station might conduct a part event at different time instants, although ideally they should happen simultaneously. In Fig. 12, we can see both the successful and the incomplete join attempts. For the latter, although some exchange of control data is achieved, no user data can be exchanged.

One can see in Fig. 12 that, when the AS flew away from the GS-SM, both stations could exchange user data until a distance of approximately 139 km between them. By contrast, when the AS flew towards the GS-SM, the user data exchange started when the AS reached a distance of 131.7 km to the GS. This difference might be caused by the different gain that the AS antenna presents in both flight directions. In addition, the

(a) From 12:58:20 to 13:18:30 UTC. The AS flies away from the GS.

(b) From 13:18:30 to 13:35:30 UTC. The AS flies towards the GS.

(c) From 13:35:30 to 13:51:16 UTC. The AS flies away from the GS.
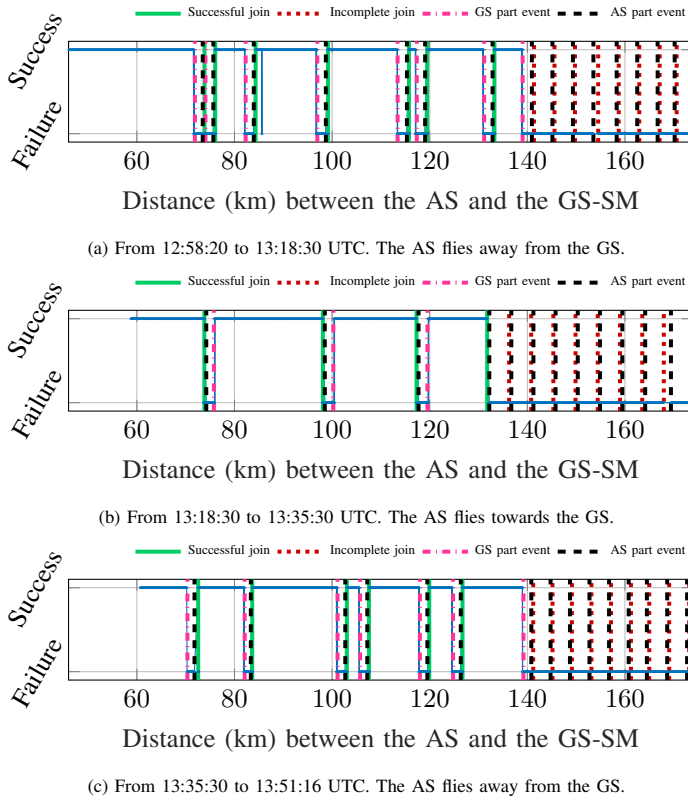
Fig. 12: Message transmissions from the AS to the GS-SM for three different flight segments of the forth flight on March 28, 2019. Messages are received by the GS either correctly (marked as Success) or incorrectly (marked as Failure), or are not be received at all (marked as Failure as well).

fact that the AS is already connected to the GS when flying away from the GS increases the communications range. This is also affected by implementation-specific timers used by the manufacturer, which are discussed in Section V-D. In general, we conclude that we could achieve an LDACS communication range of 130-140 km in the flight trials despite the limitation of the GS-EIRP to a maximum of 40 dBm and the use of a lower GS antenna gain as the one expected for GS receptions in the exemplary link budget of the LDACS specification [8]. Note that, although no user data can be exchanged from that distance, some control data messages can still be exchanged, as shown by the incomplete join events depicted in Fig. 12.

The LDACS specification does not set a minimum communication range to be achieved, but only defines the maximum designed coverage range of 200 NM and the maximum averaged EIRP of 52 dBm, indicating additionally that the EIRP can be adjusted for each cell to achieve the desired communication range and to comply with regional restrictions [8]. Although this prevents us from comparing directly the communication range reached in our flight trials with a predefined communication range, we can assume that the maximum GS-EIRP of 52 dBm is meant to be used when the maximum designed coverage range of 200 NM is desired. Taking into account free-space path losses, a reduction of 12 dB in the EIRP would approximately quarter the achievable communication range, i.e., 50 NM (92.6 km) would be reachable with an EIRP of 40 dBm. Given the fact that we achieved a much higher communication range with the same EIRP, i.e., 130-140

km with 40 dBm, we can conclude that the measured LDACS communication range was higher than expected. It is also to be noted that RL transmissions were hindered by the use of a much lower GS antenna gain as expected for reception, i.e., approximately 5 dBi instead of 12 dBi as indicated in the exemplary link budget of the LDACS specification [8]. Consequently, we expect the higher communication ranges suggested in the LDACS specification to be feasible for the recommended EIRP levels.

D. Link Outages and Received Power

We can additionally notice in Fig. 12 several link outages that occurred as the AS flew away from the GS-SM or towards it. In order to find the cause of these outages, we measure the power of the signal transmitted by the GS-SM and received by the AS during the third flown segment. More specifically, we measure the power of the signal received in the GS-SM FL channel at 1001.5 MHz, which is composed of the GS-SM FL transmitted signal, the interference falling within the channel, and the thermal noise. We then measure the thermal noise floor power and subtract it from the measured signal power, such that only the power of the GS-SM FL transmitted signal and the interference remains. In addition, we compare the AS measured received signal power with an estimate based on the CE2R theoretical model [39], [40]. The CE2R model gives a theoretical estimate of the attenuation caused by the multi-path propagation of a wireless signal when the ground-reflected specular component interferes with the direct LoS component at reception. Both the measured signal power (orange line) and the CE2R-based estimated signal power (green line) are shown in Fig. 13, together with the experienced link outages (light red area).

First, one can see that the AS received signal power is mainly composed of a continuous component, i.e., the GS-SM FL transmission, and frequent high-power interference, caused primarily by the DME stations operating in the region at close frequencies. The power of the GS-SM FL transmission fluctuates noticeably as the aircraft flies away from the GS, experiencing two deep signal fades at 13:36:30 and 13:38:10 UTC, which clearly led to the first two link outages. However, the signal power stabilises after these initial signal fades and does not show a clear relation with the link outages experienced later on. Therefore, we consider the latter link outages to be caused by a combination of different effects, such as the fast signal fading and the external interference, which leads to the loss of some consecutive messages and triggers a part event from one of the stations. This can actually be observed in Fig. 12, where we see that immediately after some messages are lost, the GS triggers a part event and does not try to decode the transmissions of the AS anymore. The AS, however, does not conduct the part event at the same time, but it triggers it after a fixed time gap of approximately 10 seconds. Only then assumes the AS that the connection is lost and tries to reconnect with the GS conducting a cell entry (join). This fixed time gap is caused by an implementation-specific timer of the AS radio and explains the fact that all observed link outages in Fig. 12 have the same duration.
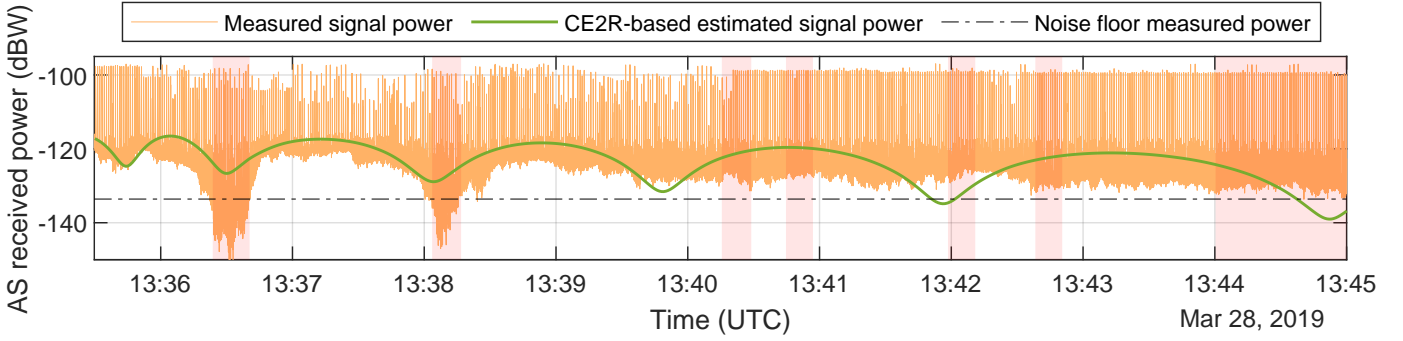
Fig. 13: Power of the GS-SM FL signal received by the AS from 13:35:30 to 13:45:00 UTC on 28 March 2019. Measured signal power (orange line) and CE2R-based estimate (green line). The time periods when the data exchange failed are shown in light red. The noise floor power (black horizontal line) has been subtracted from the GS-SM FL signal, such that only the interference and the signal transmitted by the GS-SM remain.

Although such a timer is necessary for the implementation of a data link, it must be short enough for the link to recover rapidly from short spurious outages. In addition, both stations should trigger the part events simultaneously, as any delay between them entails an unnecessary detriment of the data link performance. Therefore, we recommended the LDACS specification to provide both the compatibility criteria and detailed minimum performance thresholds to be achieved by any LDACS radio independently of its manufacturer, as well as guidance material for the implementation of data link timers.

Let us now compare the measured power of the signal received by the AS with the estimate based on the CE2R theoretical model. The CE2R-based estimated receive signal power has been obtained considering the GS-EIRP $EIRP_{GS} = 40$ dBm $= 10$ dBW, the path loss $L_{p,\text{CE2R}}$ given by the CE2R model [39], [40], and the cable losses $L_{AS} = 2$ dB between the AS antenna and the AS receiver. In addition, based on the antenna radiation pattern, an approximate antenna gain of $G_{AS} = G_{GS} = 3$ dBi can be expected for the elevation angles experienced between the GS and the AS in the shown flight segments. Consequently, the CE2R-based estimated receive signal power is obtained as

$$P_{\text{CE2R}} = EIRP_{GS} - 2 \text{ dB} - L_{p,\text{CE2R}} + G_{AS} - L_{AS},$$

where we account for the 2 dB antenna misalignment between the maximum antenna gain of 5 dBi used for the EIRP calculation and the actual antenna gain in the direction of interest.

As we can see in Fig. 13, the CE2R-based estimation of the received signal power matches quite accurately the measured signal power. The signal fading observed for distances between 60 and 90 km (between 13:35:30 and 13:39:00 UTC) are well recreated by the CE2R model. After a distance of 90 km, however, the CE2R model foresees regular signal fading events that are not actually observed in the measured signal, which flattens out and practically does not fluctuate anymore. This is actually to be expected after a certain distance, given that the grazing angle of the signal reflected on the ground decreases as the distance between the GS and the AS increases. At low grazing angles, even small building or terrain irregularities might block this ground-reflected specular component and prevent it from reaching the AS and interfering with the LoS component. However, such blockages at low grazing angles

are not considered by the CE2R model, which only considers the effect of the terrain.

We analyse now a different flight segment where the AS was connected with the GS-OP but maintained approximately the same altitude as in Fig. 13 and covered the same distances. We can see both the measured signal power and the CE2R-based estimate in Fig. 14. Again, we can see that the CE2R-based estimate matches in general quite well the measured signal power. Especially for low distances (right side of the figure, as the AS flies towards the GS), we see that both the frequency and the depth of the signal fading events are recreated with great similarity. The exact time instants (or equivalently distances), at which the signal fading events occur, do not exactly match the CE2R-based estimate. This is caused by the irregular height of the terrain between the AS and the GS, which cannot be recreated by the CE2R model and consequently prevents it from accurately predicting the reflection points. At high distances (left side of the figure), we see the same flattening in the measured signal power that we observed in Fig. 13, which is again most likely caused by the low grazing angle of the ground-reflected specular component.

We can see that the signal transmitted by GS-OP and received by the AS (Fig. 14) experienced much more frequent and sharp signal fading, compared to the signal transmitted by the GS-SM (Fig. 13). This is actually caused by the higher altitude of the GS-OP antenna, and can be well explained using the CE2R model. In principle, the phase difference between the LOS and ground-reflected components changes more quickly as the antenna height increases, triggering sharper and more frequent signal fading.

It can be concluded that the CE2R theoretical model provides an acceptable estimate of the general behaviour of the received signal in terms of its average power and the periodicity and depth of the signal fading. Unfortunately, the model can neither predict accurately the distances at which the signal fading occurs, nor recreate the presence of obstacles blocking the ground-reflected component at low grazing angles. For this to be possible, the CE2R model must be extended to take into account the specific terrain topography and the potential obstacles. Consequently, the CE2R model can be a great tool for conducting cell planning and link budget calculations but its limitations regarding the terrain irregularities and the importance of obstacles for low grazing angles should not be disregarded.
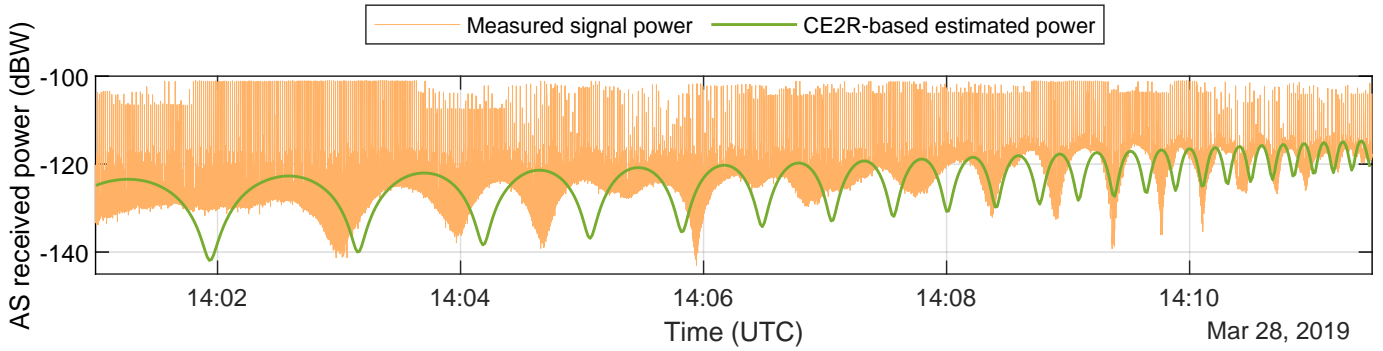
Fig. 14: Power of the GS-OP FL signal received by the AS from 14:01:00 to 14:11:30 UTC on 28 March 2019. Measured signal power (orange line) and CE2R-based estimate (green line). The noise floor power has been subtracted from the GS-OP FL signal, such that only the interference and the signal transmitted by the GS-OP remain.

It is to be noted that additional link outages arose throughout the flights when the radio LoS between the GS and AS antennas was blocked by the aircraft fuselage. As the AS antenna was mounted under the aircraft between the wings, some maneuvers performed by the aircraft during the flight trials led the aircraft fuselage to block the LoS and, consequently, resulted in a signal loss. This effect could be seen when the aircraft was rapidly ascending away from the GS or descending towards it, and especially when the aircraft was performing banking turns. Therefore, we recommend a separate investigation on possible solutions to prevent long link outages caused by aircraft maneuvers. Although some straightforward solutions are possible, such as employing one antenna on the top of the aircraft and another antenna under it, as already done by other systems, it is recommended to research on more efficient solutions minimizing the impact on the aircraft installation.

E. Quality of Service

A very important key performance indicator for quality of service is the latency of the messages containing user data. In this flight campaign, we measured the latency of each message transmitted from one station and received by its counterpart for different scenarios and traffic patterns. The latency of each message was measured from the instant when it was given to the LDACS radio of the transmit station up to the instant when it was passed on to the computer of the receiving station. Therefore, the measured latency comprises both the complete latency introduced by LDACS, including any required retransmissions, and the signal propagation between the stations. Given that the system load affects the latency introduced by the communications data link, we measured the latency of the messages transmitted in the FL (by the GS-OP and the GS-SM) and RL (by the AS) during the in-flight experiments where synthetic data following the traffic patterns T1 and T2, described in Table III, were generated and communicated through LDACS in addition to the data generated by the running applications.

The 50th, 95th, and 99th percentiles of the measured message latency of the synthetic data in both in-flight scenarios, T1 (experiments 6, 8, and 11) and T2 (experiments 7, 10, 12, and 13), are shown in Table IV. For the T1 scenario, one can see that the high-priority messages achieved a significantly

TABLE IV: Measured latency percentiles of the messages transmitted in flight in the FL and RL during the T1 (experiments 6, 8, and 11) and T2 (experiments 7, 10, 12, and 13) scenarios.

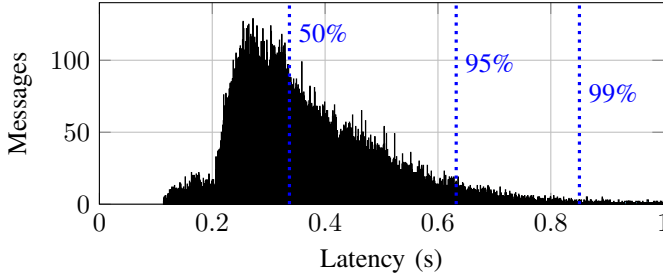| Scenario	Messages priority / size	Latency percentiles (ms)					
		50%		95%		99%	
		FL	RL	FL	RL	FL	RL
T1	High / 1400 B	99.8	177.9	310.8	426.9	433.7	579.9
	Low / 1400 B	114.4	332.9	358.0	736.8	520.9	1064.8
T2	High / 175 B	59.6	79.6	111.7	237.3	255.9	324.8
	Low / 1400 B	108.5	336.8	340.1	632.3	496.8	850.7

lower latency than the low-priority messages in both the FL and the RL for any measured percentile, despite the messages being equally sized (1400 bytes per message) in both cases. We see a much higher difference between the latency of high-priority and low-priority messages in the T2 scenario, where the message sizes differ significantly. Whilst the latency of the low-priority messages varies only slightly between the T1 and T2 scenarios, the latency of the high-priority messages is much lower in the T2 scenario in both the FL and the RL. This is reasonable given that the size of the high-priority messages is in this case reduced to 175 bytes per message. Comparing the measured latency of the FL and RL, we can notice that a message transmitted by a GS will in general present a significantly lower latency than the same message transmitted by an AS. Additionally, messages transmitted by an AS will be much more influenced by their given priorities than messages transmitted by a GS, which is understandable given the longer medium access times of the RL. Given that the T2 scenario represents the ATC+AOC data traffic expected to be covered by LDACS in the future, the results shown in Table IV for this scenario are of special importance for LDACS, as they demonstrate that LDACS can effectively prioritize the safety-relevant ATC traffic over the less critical AOC traffic in a realistic scenario.

As an example, the specific results for the messages transmitted in flight by the AS in the T2 scenario are additionally shown in Fig. 15, where histograms of the measured message latency are shown in Fig. 15a for the synthetic data with high priority, and in Fig. 15b for the synthetic data with low priority. One can clearly see that the messages representing ATC traffic (Fig. 15a) are communicated over LDACS much more quickly than the messages representing AOC traffic (Fig. 15b).

Moreover, we can notice in Fig. 15a the influence of the LDACS prioritization mechanism on communication la-
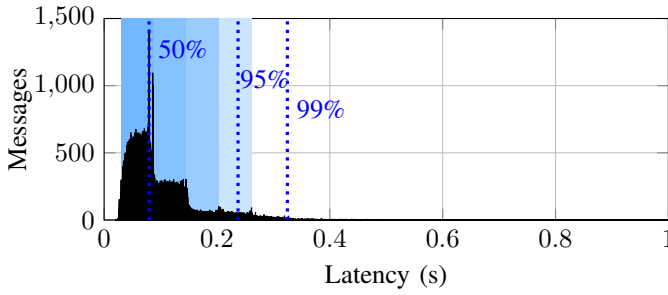
(a) Synthetic data: 116 420 high-priority messages of 175 bytes each. The blue rectangles have a width of 58.32 ms (multi-frame duration).

(b) Synthetic data: 49 724 low-priority messages of 1400 bytes each.

Fig. 15: Histogram of the latency of messages transmitted by the AS in flight during the T2 scenario. The blue dotted lines depict the 50th, 95th, and 99th latency percentiles. The high-priority messages of 175 bytes each (Fig. 15a) represent the ATC traffic and the low-priority messages of 1400 bytes each (Fig. 15b) represent traffic with a lower priority, such as AOC traffic.

tency. As schematized in Fig. 16, LDACS organizes RL transmissions into multi-frames of 58.32 ms each, in which OFDM tiles can be sent on the data channel or the dedicated control channel. This introduces a pattern into the observed latency, since user data transmissions have to be requested using the dedicated control channel. Transmission requests include the priority of the message and are answered by the GS with resource allocations in the common control channel on the FL. The resource allocations are computed from the received resource requests in order of priority. This results in a clustering of RL transmissions into integral numbers of multi-frames depending on the time until a resource request is granted by the GS. High priority requests are served first and low priority requests are served second. We can observe the clustering in the blue rectangles depicted in Fig. 15a, which have a width of 58.32 ms (multi-frame duration) each. The initial delay of half a multi-frame is due to the minimum access delay from the reception of a resource allocation in the FL common control channel to the start of the RL data slot. This effect is less visible in Fig. 15b since large packets are fragmented into smaller packets for transmission. Prioritization is clearly visible when comparing Fig. 15a and Fig. 15b.

F. Maximum Throughput with Basic Coding and Modulation

The experiments implemented only the most robust coding and modulation defined in the LDACS specification: QPSK with coding rate 1/2. Although the prototypes could consequently not reach the maximum data throughput of 2.8 Mbps, it is nevertheless instructive to analyze the maximum throughput.
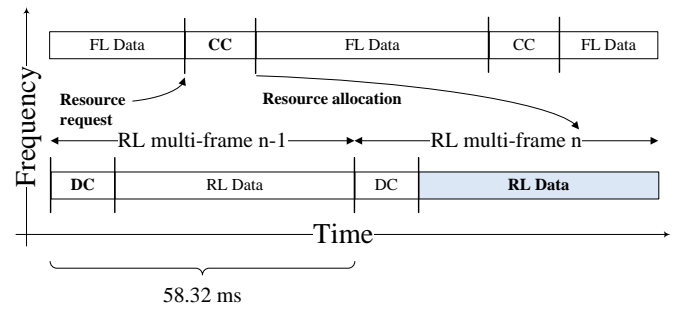

Fig. 16: The LDACS RL medium access mechanism is based on resource requests sent in the DC and resource allocations in the CC. Resource requests contain the priority of the request and are served by resource allocations in order of precedence. Resource allocations indicate user data transmission opportunities for the AS in the RL data slot.

The LDACS FL multi-frame consists of 27 FL Physical Layer Protocol Data Units (PHY-PDUs), i.e., three PHY-PDUs per OFDM frame, of 728 bit each at the implemented coding and modulation rate. In the tested configuration, two FL PHY-PDUs are used for the common control data. The expected FL user data rate provided by the remaining 25 FL PHY-PDUs is thus 303.33 kbps.

On the RL we have an additional limitation. The LDACS prototype implementation used in the flight trials could only use 110 out of 162 RL half-bandwidth tiles per multi-frame. Out of these 110 half-bandwidth tiles, two were reserved for synchronization and automatic gain control, and one was used for the dedicated control channel. Thus, 107 tiles, with a capacity of 112 bit each (at the implemented coding and modulation rate), were available for the data channel. A quick calculation shows that this results in a maximum data rate of 199.73 kbps on the RL.

The maximum throughput of LDACS was measured in the lab during the equipment integration. The AS and one GS were connected with an RF cable emulating near-perfect channel conditions. LDACS was configured to use the acknowledged transmission mode for point-to-point transmissions. However, due to the interference-free laboratory conditions, no retransmissions were observed. The data throughput of the LDACS system was measured under increasing offered load: Fourteen measurement points from 40 kbps to 310 kbps average offered load were used to drive the system into overload. User data packets were generated with constant size (1400 bytes) and exponentially-distributed inter-arrival times. Three priorities were assigned randomly and uniformly distributed to the packets resulting in three streams of packets with high/medium/low priority. Each of the fourteen measurements was repeated ten times and the reported results represent the average measurements with 95% confidence intervals.

The measured FL data throughput depicted in Fig. 17a shows clearly how the throughput increases with the offered load until the system begins to enter saturation at approximately 300 kbps offered load, as expected. The graphs of the three different priorities show that the lowest priority is the first priority to suffer losses with building overload. This effect is much more clearly visible in the RL results in Fig. 17b. Up to the expected saturation point of approximately 200 kbps offered load, all three priorities are served equally.

After the saturation point, first the lowest priority packets begin to fill up their transmission queue and are eventually dropped by the system to serve the higher priorities. Finally, the highest priority begins to push out the second priority packets, too. Note that in the case of transient overload the low priority packets would not be dropped, but stored in their transmission queue until the high priority packets have been served. However, in the artificial overload situation created by this experiment, the system is served an infinite number of high priority packets leading to the eventual time-out and drop of low priority packets.

The effect of overload to the communication latency is similar: High priority packets experience no additional latency under load since lower priority packets are pushed back in the queue. As discussed in Section II, not having a similar priority mechanism causes disruptions in the ATC communications conducted over VDL-M2 [41]. In addition, LDACS can fully utilize its theoretical throughput without suffering from medium-access losses contrary to contention-based systems like VDL-M2 used today. Due to the scarcity of aeronautical spectrum this is a major advancement.

G. Interference with Legacy Systems

Throughout the campaign, we observed DME transmissions periodically at different frequencies. As an example, we show in Fig. 18 the experimental FL band as received by the AS during some seconds of the last flight. In addition to the transmissions from the 4 GSs at 992.5, 994, 1000, and 1001.5 MHz, we can also clearly see many powerful DME transponder transmissions at 993, 997, and 999 MHz. As we showed in Fig. 6, the DME operation at these frequencies was expected and taken into account in the frequency planning. One can also see in Fig. 6 the poor spectrum utilization of the DME system, as entire parts of the spectrum are always blocked for DME but only utilized scarcely by it.

As a condition for LDACS to be allowed to operate in the L-band during the flight trials, the operation of other legacy systems was monitored throughout the entire campaign. Whilst the aircraft pilots monitored the operation of the on-board systems including DME, the agency responsible for air traffic control in Germany, *Deutsche Flugsicherung GmbH*, supervised the presence of disruptions in the operation of the deployed DME network in Germany. Despite the fact that many DME stations operated throughout the flight campaign using frequencies very close to LDACS transmissions, as shown in Fig. 6 and Fig. 18, no interference on the operation of DME was reported neither from the pilots nor from *Deutsche Flugsicherung GmbH*. Therefore, we can presume that the conducted LDACS frequency planning effectively safeguarded the operation of DME and, consequently, showed that LDACS can operate in the L-band without any impact towards DME if a careful frequency planning is conducted.

VI. CONCLUSION

This paper describes the first in-flight LDACS demonstration that took place in March and April 2019 in Germany. In addition to demonstrating the correct operation of
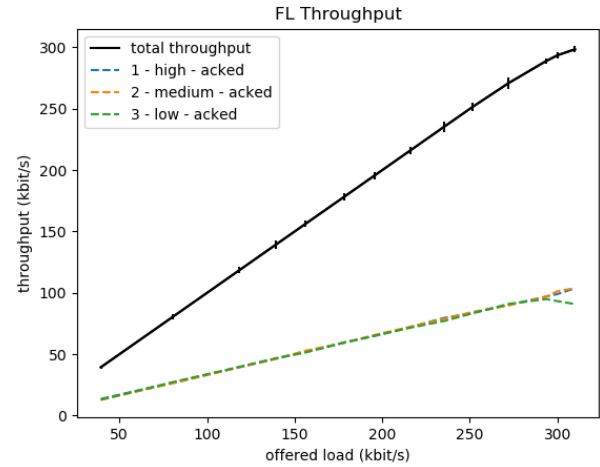
(a) FL throughput under increasing load. The prototype implementation reaches its maximum throughput at approximately 300 kbps as expected for the basic modulation and coding employed.
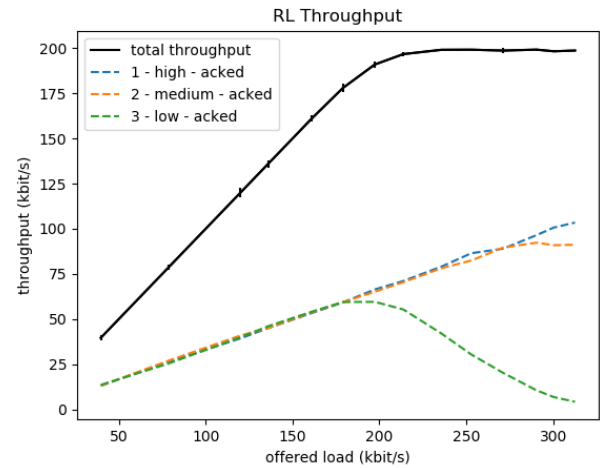
(b) RL throughput under increasing load. The prototype implementation reaches its maximum throughput at approximately 200 kbps as expected for the basic modulation and coding employed.

Fig. 17: Measured data throughput of the LDACS prototype implementation.

LDACS, this flight campaign showed that LDACS is able to support the operation of ATM-relevant applications, such as CPDLC, ADS-C, GBAS, as well as additional audio and data communications. Moreover, these applications were secured using advanced security measures: symmetric data encryption for point-to-point communications including CPDLC, ADS-C, and audio transmissions, and the TESLA protocol for GBAS broadcasts. We conclude that the high data throughput provided by LDACS allows it to support the operation of applications with diverse requirements, and enables the use of advanced security measures to protect those applications. The conducted flight trials also allowed us to measure for the first time the in-flight communication performance of LDACS, including the communication range and user data latency. The results indicate that LDACS can support RCP400/A2, RCP240, and RCP130/A1 operations, as well as RSP400/A1 and RSP180/D surveillance operations, as required by the LDACS SARPs. The exchange of synthetic data between the GSs and the AS also allowed us to test the QoS supported
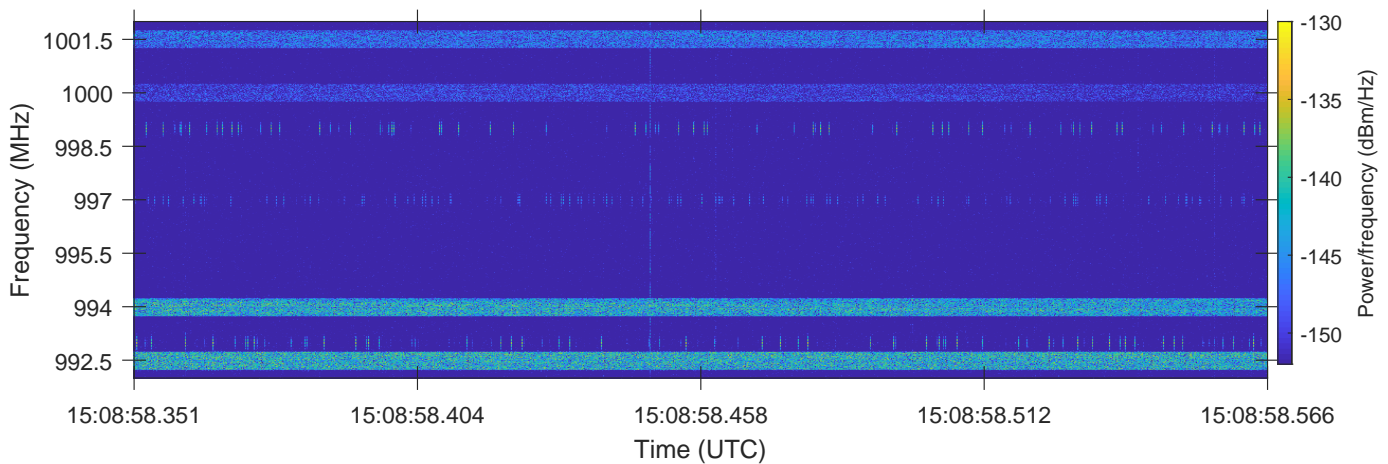
Fig. 18: Spectrogram of the experimental FL band as received by the AS on 2 April 2019. The continuous FL transmissions from the GSs can be seen at 992.5, 994, 1000, and 1001.5 MHz. Note the DME transponder transmissions at 993, 997, and 999 MHz.

by LDACS and to demonstrate that LDACS can effectively prioritize safety-relevant data, such as ATC data, over less relevant data, achieving a much lower latency for the former. Moreover, we assessed the capability of the CE2R theoretical model to recreate the path loss and signal fading accurately. Finally, no disruption in the operation of any monitored DME station in Germany was reported, which firmly corroborates that LDACS and DME can correctly operate in the same frequency band if a careful frequency planning is conducted. As a harmless operation of LDACS is a prerequisite for its deployment, providing evidence that such an operation is feasible is an important result of this flight campaign and represents a major accomplishment for LDACS.

ACRONYMS

ADS-C   Automatic Dependent Surveillance - Contract
AEEC   Airlines Electronic Engineering Committee
AES   Advanced Encryption Standard
AM(R)S   Aeronautical Mobile (Route) Service
AOC   Airline Operational Control
AS   Airborne Station
ATC   Air Traffic Control
ATM   Air Traffic Management
ATN   Aeronautical Telecommunication Network
CE2R   Curved-Earth Two-Ray
CM   Context Management
CNS   Communication, Navigation, and Surveillance
CPDLC   Controller–Pilot Data Link Communications
CSMA   Carrier-Sense Multiple Access
DLR   German Aerospace Center
DME   Distance Measuring Equipment
EIRP   Equivalent Isotropically Radiated Power
EUROCAE   European Organization for Civil Aviation Equipment
FAA   Federal Aviation Administration
FFF   Form Fit and Function
FL   Forward Link
GBAS   Ground-Based Augmentation System
GNSS   Global Navigation Satellite System

GS   Ground Station
HPA   High-Power Amplifier
ICAO   International Civil Aviation Organization
IETF   Internet Engineering Task Force
IP   Internet Protocol
LDACS   L-band Digital Aeronautical Communications System
LNA   Low-Noise Amplifier
LoS   Line of Sight
MAC   Message Authentication Code
MASPS   Minimum Aviation System Performance Specifications
MOPS   Minimum Operational Performance Standards
OFDM   Orthogonal Frequency-Division Multiplexing
PHY-PDUs   Physical Layer Protocol Data Units
PQC   Post-Quantum Cryptography
QoS   Quality of Service
RCP   Required Communication Performance
RL   Reverse Link
RSP   Required Surveillance Performance
RTCA   Radio Technical Commission for Aeronautics
SARPS   Standards and Recommended Practices
SESAR   Single European Sky ATM Research
TESLA   Timed Efficient Stream Loss-tolerant Authentication
VDL-M2   VHF Data Link - Mode 2

APPENDIX A
CONDUCTED EXPERIMENTS

Table V describes the experiments conducted in the flight trials, including the beginning and ending of the experiments, the performed tests, and the demonstrated applications. The experiments were conducted in flight, with the exception of the experiments 1, 9, 22, and 25, which took place with the aircraft on the airport apron. All data were exchanged using the LDACS acknowledged mode. Any user data, i.e., synthetic and from applications, were only exchanged between the AS and a GS when the AS was connected to it. During the handover tests, the exchange of application data between the AS and a GS was paused every time the AS left the cell, and resumed when the AS rejoined it.

This article has been accepted for publication in a future issue of this journal, but has not been fully edited. Content may change prior to final publication. Citation information: DOI 10.1109/TAES.2021.3111722, IEEE Transactions on Aerospace and Electronic Systems

17

TABLE V: Description of the conducted experiments.

Exp.	Flight	Start (UTC)	End (UTC)	Tests and Applications
1	1	8:19:18	8:32:08	Secure GBAS, secure CPDLC, secure ADS-C, and secure audio transmission between AS and GS-OP.
2	1	8:43:03	9:43:33	Secure GBAS, secure CPDLC, secure ADS-C, and secure audio transmission between AS and GS-OP.
3	1	9:48:05	9:58:55	Secure GBAS between AS and GS-OP. AS handover tests between GS-OP and GS-SM.
4	1	10:01:42	10:26:32	Secure GBAS, secure CPDLC, and secure ADS-C between AS and GS-OP.
5	1	10:28:37	10:53:16	Secure GBAS, secure CPDLC, and secure ADS-C between AS and GS-OP.
6	2	9:03:57	9:37:12	Test of the T1 data traffic scenario (see Table III) between AS and GS-OP. Concurrently secure CPDLC and secure ADS-C between AS and GS-OP.
7	2	9:39:06	9:52:48	Test of the T2 data traffic scenario (see Table III) between AS and GS-SM. Concurrently secure CPDLC and secure ADS-C between AS and GS-SM.
8	2	9:55:00	10:34:17	Test of the T1 data traffic scenario (see Table III) between AS and GS-OP. Concurrently secure CPDLC and secure ADS-C between AS and GS-OP.
9	2	10:35:25	10:45:15	Test of the T1 data traffic scenario (see Table III) between AS and GS-OP. Concurrently secure ADS-C between AS and GS-OP.
10	3	12:57:05	14:09:38	Test of the T2 data traffic scenario (see Table III) between AS and GS-OP. Concurrently secure CPDLC and secure ADS-C between AS and GS-OP.
11	3	14:13:07	15:05:35	Test of the T1 data traffic scenario (see Table III) between AS and GS-SM.
12	3	15:08:26	15:41:08	Test of the T2 data traffic scenario (see Table III) between AS and GS-OP. Concurrently secure CPDLC and secure ADS-C between AS and GS-OP.
13	3	15:42:17	16:01:03	Test of the T2 data traffic scenario (see Table III) between AS and GS-OP. Concurrently secure CPDLC and secure ADS-C between AS and GS-OP.
14	4	11:03:14	11:25:01	Long range test with GS-OP. Secure CPDLC and secure ADS-C between AS and GS-OP.
15	4	11:25:54	11:37:14	Long range test with GS-OP. Secure CPDLC and secure ADS-C between AS and GS-OP.
16	4	11:44:20	11:50:38	Long range test with GS-OP.
17	4	11:51:46	12:03:49	Long range test with GS-OP.
18	4	12:04:22	12:05:59	Long range test with GS-SM.
19	4	12:06:28	12:48:27	Long range test with GS-OP. Secure CPDLC and secure ADS-C between AS and GS-OP.
20	4	12:50:38	13:51:16	Long range test with GS-SM.
21	4	13:54:45	14:42:03	Long range test with GS-OP. Secure CPDLC and secure ADS-C between AS and GS-OP.
22	5	9:18:04	9:25:09	Secure CPDLC between AS and GS-OP.
23	5	9:25:46	9:33:10	AS handover tests between GS-OP and GS-SM. Secure CPDLC between AS and GS-OP.
24	5	9:35:58	11:04:36	AS handover tests between GS-OP and GS-SM. Secure CPDLC and secure ADS-C between AS and GS-OP. Open CPDLC between AS and both GS-OP and GS-SM.
25	5	11:36:09	12:30:40	Test of the T2 data traffic scenario (see Table III) between AS and GS-OP.
26	6	14:06:28	14:27:16	Open GBAS, secure CPDLC, secure ADS-C, and open CPDLC between AS and GS-OP.
27	6	14:29:22	15:18:35	Secure GBAS, open GBAS, secure CPDLC, secure ADS-C, and open CPDLC between AS and GS-OP.
28	6	15:20:06	16:10:58	Secure GBAS, secure CPDLC, secure ADS-C, and open CPDLC between AS and GS-OP.

APPENDIX B
THE MICONAV PROJECT

The flight campaign was performed as part of the MI-CONAV project, a research project receiving national funding from the research program LuFo V-2 (*Luftfahrtforschungsprogramm*) of the German Federal Ministry of Economy and Energy (BMWi). The goal of the project was to develop full duplex LDACS demonstrators as defined by the LDACS specification and to realize them using industrial development methods. MICONAV built on the results of two previous projects: ICONAV [42] and LDACS-NAV [43]. It was conducted in liaison with SESAR2020 and its results were communicated to EUROCONTROL and ICAO. The organizations composing the MICONAV consortium are Rohde & Schwarz GmbH & Co. KG, the German Aerospace Center (DLR, Deutsches Zentrum für Luft- und Raumfahrt e.V.), iAd Gesellschaft für Informatik, Automatisierung und Datenverarbeitung mbH, and BPS GmbH.

ACKNOWLEDGMENTS

REFERENCES

[1] Industry High Level Group (IHLG), "Aviation Benefits Report," 2019. [Online]. Available: https://www.icao.int/sustainability/Documents/AVIATION-BENEFITS-2019-web.pdf

[2] STATFOR, "European Aviation in 2040. Challenges of Growth. Annex 1: Flight Forecast to 2040," EUROCONTROL, 2018.

[3] International Civil Aviation Organization, "Doc 9718: Handbook on Radio Frequency Spectrum Requirements for Civil Aviation, Volume I, ICAO spectrum strategy, policy statements and related information," second edition, 2018.

[4] EUROCONTROL, "Radio Frequency Function 2020 report," first edition, March 2021.

[5] EUROCONTROL/FAA, "Action Plan 17 - Future Communications Study: Final Conclusions and Recommendations Report," EUROCONTROL/FAA Memorandum of Cooperation, Tech. Rep, 2007.

[6] SESAR JU, "European ATM Master Plan," 2020. [Online]. Available: https://www.atmmasterplan.eu/

[7] International Civil Aviation Organization, "2016-2030 Global Air Navigation Plan," 2016.

[8] T. Gräupl, C. Rihacek, B. Haindl, and Q. Parrod, "LDACS A/G Specification," SESAR2020, Tech. Rep. PJ14-02-01 D3.3.030, Aug. 2019. [Online]. Available: https://www.ldacs.com/

[9] T. Gräupl and M. Ehammer, "LDACS1 data link layer evolution for ATN/IPS," in *Proc. IEEE/AIAA 30th Digital Avionics Systems Conf. (DASC)*, Seattle, WA, USA, Oct. 2011, p. 16.

[10] C. Rihacek, M. Sajatovic, J. Meser, and T. Gräupl, "L-band Digital Aeronautical Communications System (LDACS) - Technical Validations in SESAR2020," in *Proc. IEEE/AIAA 38th Digital Avionics Systems Conf. (DASC)*, San Diego, CA, USA, Sep. 2019.

[11] M. A. Bellido-Manganell, T. Gräupl, and M. Schnell, "Impact Assessment of the L-Band Digital Aeronautical Communications System on the Joint Tactical Information Distribution System," *IEEE Transactions on Vehicular Technology*, vol. 68, no. 4, pp. 3629–3641, Apr. 2019.

[12] B. Haindl, J. Meser, M. Sajatovic, S. Müller, H. Arthaber, T. Faseth, and M. Zaisberger, "LDACS1 Conformance and Compatibility Assessment,"

This article has been accepted for publication in a future issue of this journal, but has not been fully edited. Content may change prior to final publication. Citation information: DOI 10.1109/TAES.2021.3111722, IEEE Transactions on Aerospace and Electronic Systems

18

in *Proc. IEEE/AIAA 33rd Digital Avionics Systems Conf. (DASC)*, Colorado Springs, CO, USA, Oct. 2014, p. 11.

[13] M. Mostafa, M. A. Bellido-Manganell, and T. Gräupl, "Feasibility of Cell Planning for the L-Band Digital Aeronautical Communications System Under the Constraint of Secondary Spectrum Usage," *IEEE Transactions on Vehicular Technology*, vol. 67, no. 10, pp. 9721–9733, Oct. 2018.

[14] International Civil Aviation Organization, "Finalization of LDACS Draft SARPs," Second Meeting of DCIWG (Data Communication Infrastructure Working Group), Montreal, Tech. Rep. Working Paper WP05 including Appendix, Oct. 2018.

[15] B. Biswas and N. Sendrier, "McEliece Cryptosystem Implementation: Theory and Practice," in *International Workshop on Post-Quantum Cryptography*. Springer, 2008, pp. 47–62.

[16] H. Bartz and G. Liva, "On Decoding Schemes for the MDPC-McEliece Cryptosystem," in *12th International ITG Conference on Systems, Communications and Coding (SCC)*. Rostock, Germany: VDE, Feb. 2019, pp. 245–250.

[17] A. Perrig, R. Canetti, J. D. Tygar, and D. Song, "The TESLA Broadcast Authentication Protocol," *Rsa Cryptobytes*, vol. 5, no. 2, pp. 2–13, 2002.

[18] N. Mäurer, T. Gräupl, and C. Schmitt, "L-band Digital Aeronautical Communications System (LDACS)," Working Draft, IETF Secretariat, Internet-Draft draft-maeurer-raw-ldacs-08, May 2021. [Online]. Available: https://www.ietf.org/archive/id/draft-ietf-raw-ldacs-08.txt

[19] M. Carandente and C.-H. Rokitansky, "VDL Mode 2 Capacity and Performance Analysis," SESAR JU, Tech. Rep. SESAR-CFT-0096, November 2015. [Online]. Available: https://www.sesarju.eu/sites/default/files/documents/news/SJU_VDL_Mode_2_Capacity_and_Performance_Analysis.pdf

[20] International Civil Aviation Organization, "Doc 9869: Performance-based Communication and Surveillance (PBCS) Manual," second edition, 2017.

[21] RTCA SC-214, "Safety and Performance Requirements Standard for Baseline 2 ATS Data Communications (Baseline 2 SPR Standard)," RTCA, Tech. Rep. RTCA DO-350A, 2016.

[22] N. Schneckenburger, T. Jost, D. Shutin, M. Walter, T. Thiasiriphet, M. Schnell, and U.-C. Fiebig, "Measurement of the L-band Air-to-Ground Channel for Positioning Applications," *IEEE Transactions on Aerospace and Electronic Systems*, vol. 52, no. 5, pp. 2281–2297, 2016.

[23] A. Filip and D. Shutin, "Ambiguity Function Analysis for OFDM-Based LDACS Passive Multistatic Radar," *IEEE Transactions on Aerospace and Electronic Systems*, vol. 54, no. 3, pp. 1323–1340, 2017.

[24] M. A. Bellido-Manganell, "Design Approach of a Future Air-to-Air Data Link," in *Proc. IEEE/AIAA 38th Digital Avionics Systems Conf. (DASC)*, London, UK, Sept. 2018.

[25] M. A. Bellido-Manganell and M. Schnell, "Towards Modern Air-to-Air Communications: the LDACS A2A Mode," in *Proc. IEEE/AIAA 38th Digital Avionics Systems Conf. (DASC)*, San Diego, CA, USA, Sept. 2019.

[26] D. Shutin, N. Schneckenburger, M. Walter, T. Thiasiriphet, N. Franzen, A. Filip, and M. Schnell, "LDACS1 ranging results with Doppler smoothing from new flight experiments," in *Proc. IEEE/AIAA 33rd Digital Avionics Systems Conference (DASC)*, Colorado Springs, CO, USA, Oct. 2014, pp. 3C1–1.

[27] O. Osechas, S. Narayanan, O. Garcia Crespillo, G. Zampieri, G. Battista, R. Kumar, N. Schneckenburger, E. Lay, B. Belabbas, and M. Meurer, "Feasibility Demonstration of Terrestrial RNP with LDACS," in *Proc. 32nd International Technical Meeting of the Satellite Division of The Institute of Navigation (ION GNSS+ 2019)*, Miami, Florida, USA, Sept. 2019.

[28] International Civil Aviation Organization, "Doc 9776: Manual on VHF Digital Link (VDL) Mode 2," first edition, 2001.

[29] A. Roy, "VDL Systems: Current Status in the USA and Spectrum Considerations for Potential Future VDL Systems," International Civil Aviation Organization, Thirty-Third Meeting of the Frequency Spectrum Management Panel (FSMP) Working Group F (Frequency), Montreal, Canada, August 2015.

[30] M. Felux, T. Gräupl, N. Mäurer, and M. Stanisak, "Transmitting GBAS Messages via LDACS," in *Proc. IEEE/AIAA 37th Digital Avionics Systems Conf. (DASC)*, London, UK, Sept. 2018.

[31] N. Mäurer, T. Gräupl, M. A. Bellido-Manganell, D. M. Mielke, A. Filip-Dhaubhadel, O. Heirich, D. Gerbeth, M. Felux, L. M. Schalk, D. Becker, N. Schneckenburger, and M. Schnell, "Flight Trial Demonstration of Secure GBAS via the L-band Digital Aeronautical Communications System (LDACS)," *IEEE Aerospace and Electronic Systems Magazine*, vol. 36, no. 4, pp. 8–17, 2021.

[32] N. Mäurer and A. Bilzhause, "A Cybersecurity Architecture for the L-band Digital Aeronautical Communications System (LDACS)," in *Proc. IEEE/AIAA 37th Digital Avionics Systems Conf. (DASC)*, London, UK, USA, Sept. 2018.

[33] N. Mäurer and C. Schmitt, "Towards Successful Realization of the LDACS Cybersecurity Architecture: An Updated Datalink Security Threat- and Risk Analysis," in *Proc. IEEE Integrated Communications, Navigation and Surveillance Conference (ICNS)*, Herndon, VA, USA, Apr. 2019, pp. 1A2–1–1A2–13.

[34] D. McGrew and J. Viega, "The Galois/Counter Mode of Operation (GCM)," *submission to NIST Modes of Operation Process*, vol. 20, 2004.

[35] D. McGrew and K. Igoe, "AES-GCM Authenticated Encryption in the Secure Real-time Transport Protocol (SRTP)," RFC 7714 (Standards Track), Internet Engineering Task Force, 2015.

[36] E. Barker, "Recommendation for Key Management: Part 1 - General," National Institute of Standards and Technology (NIST), Gaithersburg, MD, USA, NIST Special Publication 800-57 Part 1 Revision 5, May 2020. [Online]. Available: https://nvlpubs.nist.gov/nistpubs/SpecialPublications/NIST.SP.800-57pt1r5.pdf

[37] N. Mäurer, T. Gräupl, and C. Schmitt, "Evaluation of the LDACS Cybersecurity Implementation," in *Proc. IEEE/AIAA 38th Digital Avionics Systems Conference (DASC)*, San Diego, CA, USA, Sept. 2019.

[38] N. Mäurer, T. Gräupl, and C. Schmitt, "Comparing Different Diffie-Hellman Key Exchange Flavors for LDACS," in *Proc. IEEE/AIAA 39th Digital Avionics Systems Conference (DASC)*, San Antonio, TX, USA (virtual conference), Oct. 2020.

[39] D. W. Matolak and R. Sun, "Unmanned Aircraft Systems: Air-Ground Channel Characterization for Future Applications," *IEEE Vehicular Technology Magazine*, vol. 10, no. 2, pp. 79–85, 2015.

[40] ——, "Air–Ground Channel Characterization for Unmanned Aircraft Systems—Part I: Methods, Measurements, and Models for Over-Water Settings," *IEEE Transactions on Vehicular Technology*, vol. 66, no. 1, pp. 26–44, 2016.

[41] A. Kanstein, "VDL Mode 2 Measurement, Analysis and Simulation Campaign," SESAR2020, Tech. Rep. SJU/LC/0109-CFT – D1602, Report D11, 2016. [Online]. Available: https://www.eraa.org/system/files/elsa_vdlm2_final_data_link_study_0.pdf

[42] "ICONAV project homepage: http://www.dlr.de/kn/desktopdefault.aspx/tabid-4309/3222_read-36946."

[43] "LDACS-NAV project homepage: http://www.dlr.de/kn/desktopdefault.aspx/tabid-4309/3222_read-35386."

Miguel A. Bellido Manganell received his B.Sc./M.Sc degrees in telecommunication engineering from University of Granada and University of Malaga, Spain, in 2014/2016. In 2016 he joined the Institute of Communications and Navigation of the German Aerospace Center (DLR) as a research associate in the Aeronautical Communications group. He has participated in several flight and measurement campaigns and had a leading role in the 2019 LDACS flight campaign MICONAV. His current research focus is on channel modeling, physical layer design and digital signal processing in aeronautical wireless communications, as well as medium access control in ad hoc networks. Miguel A. Bellido Manganell was the recipient of multiple prizes, including the award for the best academic trajectory in telecommunication engineering of Malaga City Council, Spain, in 2017, the best master thesis and the outstanding end-of-studies awards of the M.Sc. degree in telecommunication engineering 2015/2016 of the University of Malaga, Spain, as well as awards at research conferences.

This article has been accepted for publication in a future issue of this journal, but has not been fully edited. Content may change prior to final publication. Citation information: DOI 10.1109/TAES.2021.3111722, IEEE Transactions on Aerospace and Electronic Systems

19

Thomas Gräupl received the Ph.D. degree in computer science and the M.Sc degree in mathematics from the University of Salzburg, Austria in 2011 and 2004, respectively. He is a researcher with the institute of communications and navigation of the German Aerospace Center DLR. He was a researcher with the University of Salzburg. His current research interests include wireless digital communication systems and the performance evaluation of communication systems through computer simulations.

Lukas Marcel Schalk received his B.Sc. degree in General Engineering Science and his M.Sc. degree in Electrical Engineering from Hamburg University of Technology, Germany, in 2013 and 2015, respectively. Since 2016 he has been a scientific researcher at the Institute of Communications and Navigation of the German Aerospace Center (DLR). His research interests include aeronautical communication systems, especially for command, control and cooperative surveillance of unmanned aircraft.

Oliver Heirich studied electrical engineering at the University Ulm in Germany and graduated as Dipl.-Ing. in 2008. He received the Ph.D. degree in electrical engineering in 2020 from Technische Universität Munich (TUM). In 2008, he worked as an electronic development engineer at an industrial sensor manufacturer. Since 2010, he is a research engineer at the Institute of Communications and Navigations at the German Aerospace Center (DLR) in Oberpfaffenhofen, Germany. His research focuses mainly on multi-sensor navigation with GNSS, IMU, magnetic sensors and maps, especially for railway applications.

Dennis Becker received his Bachelor and Master degrees in Electrical Engineering from Duale Hochschule Baden-Württemberg in 2011 and from Technische Universität Darmstadt in 2014 respectively. He continued studying Information and Communications Engineering and obtained his second Master degree in 2017. In January 2018, Dennis joined the Institute of Communication and Navigation at the German Aerospace Center (DLR) as a research assistant in the Aeronautical Communications group. His current research focus is on analyzing the communications channel between small sized unmanned aerial vehicles.

Nils Mäurer has been working as a scientist at the Institute of Communications and Navigation for the German Aerospace Center (DLR) since 2017. There he is researching the cybersecurity design of LDACS. In the 2019 LDACS flight campaign MICONAV, he was directly responsible for the worldwide first demonstration of post-quantum secured communications in civil aviation. Also, he was directly responsible for demonstrating the worldwide first secure transmission of Ground Based Augmentation System (GBAS) data via the LDACS datalink. He won several awards at numerous conferences, such as the Best-of-Conference award at the Integrated Communications Navigation and Surveillance (ICNS) conference in 2019. Currently, he is finishing his PhD thesis at the Bundeswehr University Munich, Germany.

Nicolas Schneckenburger received his Dipl-Ing. degree in electrical engineering from the university of Ulm, Germany, in 2010 and the Doctoral degree from the Technische University Ilmenau, Germany, in 2017. From 2010 to 2019 he was working as a research associate with the Institute of Communication and Navigation at DLR (German Aerospace Center). His focus during the last years has been on new communication and navigation systems in civil aviation. In that context, he has conducted different flight measurement campaigns.

Alexandra Filip-Dhaubhadel received the bachelor's and master's degrees in electrical engineering from Jacobs University Bremen, Germany, in 2011 and 2013, respectively, and the PhD degree from the Chemnitz University of Technology in 2020. In September 2013, she joined the Institute of Communications and Navigation, German Aerospace Center (DLR) as a Research Associate in the Aeronautical Communications Group. Her current research focus is on passive multistatic radar systems and the associated radar signal processing techniques.

Michael Schnell Michael Schnell is Head of the Aeronautical Communications Research Group at the Institute of Communications and Navigation of the German Aerospace Center (DLR). The main research topics of his group are the development and modernization of CNS technologies for civil aviation and unmanned aerial systems. After his studies at the University Erlangen-Nuremberg he joined DLR in 1990 with a M.Sc. degree in electrical engineering. Since then he has been working as scientific researcher and earned a Ph.D. degree for his work on wireless communications in 1997. Dr. Schnell is a lecturer for multi-carrier communications as well as for aeronautical communications and acts as selected advisor for the German Air Navigation Service Provider (DFS GmbH) on various committees at EUROCONTROL and ICAO. As Rapporteur of the Project Team "Terrestrial Data Link" within the ICAO Communications Panel he is organizing the international LDACS standardization. He has authored/co-authored over 100 publications, including more than 20 journal articles. He is a senior member IEEE as well as member of AIAA and VDE/ITG.

Daniel M. Mielke received his B.Sc./M.Sc. from University of Kiel in 2014/2016 and spent a term at the UBC in Vancouver. He joined DLR in 2016. His research interests are channel modeling and robust wireless communication systems in aviation. He is a PhD candidate at the University of Ulm.